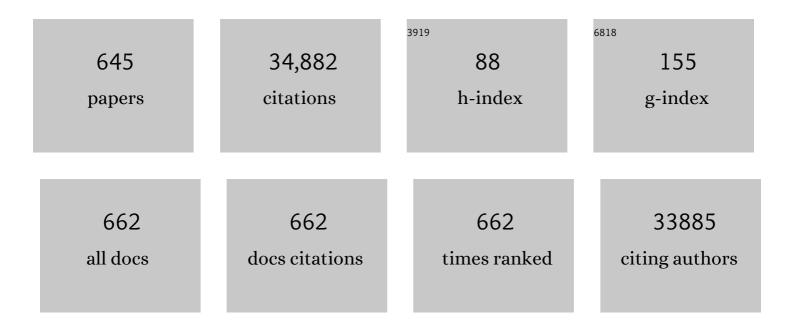


## List of Publications by Year in descending order

Source: https://exaly.com/author-pdf/665391/publications.pdf Version: 2024-02-01



VILUO

#	Article	IF	CITATIONS
1	Singleâ€Atom Pt as Coâ€Catalyst for Enhanced Photocatalytic H <sub>2</sub> Evolution. Advanced Materials, 2016, 28, 2427-2431.	11.1	1,156
2	Nickel–vanadium monolayer double hydroxide for efficient electrochemical water oxidation. Nature Communications, 2016, 7, 11981.	5.8	808
3	Occurrence and Transport of Tetracycline, Sulfonamide, Quinolone, and Macrolide Antibiotics in the Haihe River Basin, China. Environmental Science & Technology, 2011, 45, 1827-1833.	4.6	786
4	Defect-Mediated Electron–Hole Separation in One-Unit-Cell ZnIn <sub>2</sub> S <sub>4</sub> Layers for Boosted Solar-Driven CO <sub>2</sub> Reduction. Journal of the American Chemical Society, 2017, 139, 7586-7594.	6.6	764
5	Atomically dispersed platinum supported on curved carbon supports for efficient electrocatalytic hydrogen evolution. Nature Energy, 2019, 4, 512-518.	19.8	756
6	Trends in Antibiotic Resistance Genes Occurrence in the Haihe River, China. Environmental Science & Technology, 2010, 44, 7220-7225.	4.6	661
7	Single Pt Atoms Confined into a Metal–Organic Framework for Efficient Photocatalysis. Advanced Materials, 2018, 30, 1705112.	11.1	599
8	Conversion of Dinitrogen to Ammonia by FeN <sub>3</sub> -Embedded Graphene. Journal of the American Chemical Society, 2016, 138, 8706-8709.	6.6	562
9	Occurrence of sulfonamide and tetracycline-resistant bacteria and resistance genes in aquaculture environment. Water Research, 2012, 46, 2355-2364.	5.3	556
10	Boosting Photocatalytic Hydrogen Production of a Metal–Organic Framework Decorated with Platinum Nanoparticles: The Platinum Location Matters. Angewandte Chemie - International Edition, 2016, 55, 9389-9393.	7.2	513
11	Prevalence and proliferation of antibiotic resistance genes in two municipal wastewater treatment plants. Water Research, 2015, 85, 458-466.	5.3	448
12	Versatile Roomâ€Temperatureâ€Phosphorescent Materials Prepared from Nâ€Substituted Naphthalimides: Emission Enhancement and Chemical Conjugation. Angewandte Chemie - International Edition, 2016, 55, 9872-9876.	7.2	343
13	Dinitrogen Cleavage and Hydrogenation by a Trinuclear Titanium Polyhydride Complex. Science, 2013, 340, 1549-1552.	6.0	327
14	Tuning Chemical Enhancement of SERS by Controlling the Chemical Reduction of Graphene Oxide Nanosheets. ACS Nano, 2011, 5, 952-958.	7.3	324
15	How Graphene Is Cut upon Oxidation?. Journal of the American Chemical Society, 2009, 131, 6320-6321.	6.6	323
16	Ultrathin amorphous cobalt–vanadium hydr(oxy)oxide catalysts for the oxygen evolution reaction. Energy and Environmental Science, 2018, 11, 1736-1741.	15.6	310
17	Visualizing coherent intermolecular dipole–dipole coupling in real space. Nature, 2016, 531, 623-627.	13.7	284
18	Cationic Alkyl Rare-Earth Metal Complexes Bearing an Ancillary Bis(phosphinophenyl)amido Ligand: A Catalytic System for Livingcis-1,4-Polymerization and Copolymerization of Isoprene and Butadiene. Angewandte Chemie - International Edition, 2007, 46, 1909-1913.	7.2	263

#	Article	IF	CITATIONS
19	New Mechanism for Photocatalytic Reduction of CO <sub>2</sub> on the Anatase TiO <sub>2</sub> (101) Surface: The Essential Role of Oxygen Vacancy. Journal of the American Chemical Society, 2016, 138, 15896-15902.	6.6	256
20	Distinguishing adjacent molecules on a surface using plasmon-enhanced Raman scattering. Nature Nanotechnology, 2015, 10, 865-869.	15.6	239
21	Distribution, sources and composition of antibiotics in sediment, overlying water and pore water from Taihu Lake, China. Science of the Total Environment, 2014, 497-498, 267-273.	3.9	234
22	Electronic and vibronic contributions to two-photon absorption of molecules with multi-branched structures. Journal of Chemical Physics, 2000, 113, 7055-7061.	1.2	226
23	Occurrence and distribution of antibiotics, antibiotic resistance genes in the urban rivers in Beijing, China. Environmental Pollution, 2016, 213, 833-840.	3.7	226
24	lsoprene Polymerization with Yttrium Amidinate Catalysts: Switching the Regio―and Stereoselectivity by Addition of AlMe <sub>3</sub> . Angewandte Chemie - International Edition, 2008, 47, 2642-2645.	7.2	225
25	Graphene nanoribbon as a negative differential resistance device. Applied Physics Letters, 2009, 94, .	1.5	219
26	Hollow Iron–Vanadium Composite Spheres: A Highly Efficient Ironâ€Based Water Oxidation Electrocatalyst without the Need for Nickel or Cobalt. Angewandte Chemie - International Edition, 2017, 56, 3289-3293.	7.2	216
27	Unprecedented Isospecific 3,4-Polymerization of Isoprene by Cationic Rare Earth Metal Alkyl Species Resulting from a Binuclear Precursor. Journal of the American Chemical Society, 2005, 127, 14562-14563.	6.6	215
28	Tracking Structural Selfâ€Reconstruction and Identifying True Active Sites toward Cobalt Oxychloride Precatalyst of Oxygen Evolution Reaction. Advanced Materials, 2019, 31, e1805127.	11.1	211
29	Optically Switchable Photocatalysis in Ultrathin Black Phosphorus Nanosheets. Journal of the American Chemical Society, 2018, 140, 3474-3480.	6.6	210
30	Nonlocal Exchange Interaction Removes Half-Metallicity in Graphene Nanoribbons. Nano Letters, 2007, 7, 2211-2213.	4.5	202
31	Effects of ï€ centers and symmetry on two-photon absorption cross sections of organic chromophores. Journal of Chemical Physics, 2001, 114, 9813-9820.	1.2	193
32	Role of point defects on the reactivity of reconstructed anatase titanium dioxide (001) surface. Nature Communications, 2013, 4, 2214.	5.8	184
33	Spatial and temporal variations in the relationship between lake water surface temperatures and water quality - A case study of Dianchi Lake. Science of the Total Environment, 2018, 624, 859-871.	3.9	184
34	Simulations of vibronic profiles in two-photon absorption. Chemical Physics Letters, 2000, 330, 447-456.	1.2	178
35	Aggregationâ€Induced Dualâ€Phosphorescence from Organic Molecules for Nondoped Lightâ€Emitting Diodes. Advanced Materials, 2019, 31, e1904273.	11.1	177
36	Designing pâ€Type Semiconductor–Metal Hybrid Structures for Improved Photocatalysis. Angewandte Chemie - International Edition, 2014, 53, 5107-5111.	7.2	176

#	Article	IF	CITATIONS
37	Simultaneous removal of antibiotics and antibiotic resistance genes from pharmaceutical wastewater using the combinations of up-flow anaerobic sludge bed, anoxic-oxic tank, and advanced oxidation technologies. Water Research, 2019, 159, 511-520.	5.3	175
38	Molecular co-catalyst accelerating hole transfer for enhanced photocatalytic H2 evolution. Nature Communications, 2015, 6, 8647.	5.8	172
39	Realizing a Not-Strong-Not-Weak Polarization Electric Field in Single-Atom Catalysts Sandwiched by Boron Nitride and Graphene Sheets for Efficient Nitrogen Fixation. Journal of the American Chemical Society, 2020, 142, 19308-19315.	6.6	170
40	Observation of Photocatalytic Dissociation of Water on Terminal Ti Sites of TiO <sub>2</sub> (110)-1 <i>×</i> 1 Surface. Journal of the American Chemical Society, 2012, 134, 9978-9985.	6.6	160
41	A Second oordination‧phere Strategy to Modulate Nickel―and Palladium atalyzed Olefin Polymerization and Copolymerization. Angewandte Chemie - International Edition, 2017, 56, 11604-11609.	7.2	159
42	Atomicâ€Layerâ€Confined Doping for Atomicâ€Level Insights into Visibleâ€Light Water Splitting. Angewandte Chemie - International Edition, 2015, 54, 9266-9270.	7.2	158
43	Sub-nanometre control of the coherent interaction between a single molecule and a plasmonic nanocavity. Nature Communications, 2017, 8, 15225.	5.8	158
44	First-principle study of electronic and optical properties of two-dimensional materials-based heterostructures based on transition metal dichalcogenides and boron phosphide. Applied Surface Science, 2019, 476, 70-75.	3.1	154
45	Sub-nanometre resolution in single-molecule photoluminescence imaging. Nature Photonics, 2020, 14, 693-699.	15.6	152
46	Mechanism for Negative Differential Resistance in Molecular Electronic Devices: Local Orbital Symmetry Matching. Physical Review Letters, 2007, 99, 146803.	2.9	150
47	Theoretical Study on the Mechanism of Photoreduction of CO <sub>2</sub> to CH <sub>4</sub> on the Anatase TiO <sub>2</sub> (101) Surface. ACS Catalysis, 2016, 6, 2018-2025.	5.5	149
48	The occurrence and fate of tetracyclines in two pharmaceutical wastewater treatment plants of Northern China. Environmental Science and Pollution Research, 2016, 23, 1722-1731.	2.7	147
49	Effect of the selective pressure of sub-lethal level of heavy metals on the fate and distribution of ARGs in the catchment scale. Environmental Pollution, 2017, 220, 900-908.	3.7	144
50	Enhanced Asymmetric Induction for the Copolymerization of CO <sub>2</sub> and Cyclohexene Oxide with Unsymmetric Enantiopure SalenCo(III) Complexes: Synthesis of Crystalline CO <sub>2</sub> -Based Polycarbonate. Journal of the American Chemical Society, 2012, 134, 5682-5688.	6.6	140
51	Ammonia formation by a thiolate-bridged diiron amide complex as a nitrogenase mimic. Nature Chemistry, 2013, 5, 320-326.	6.6	139
52	Unraveling Surface Plasmon Decay in Core–Shell Nanostructures toward Broadband Light-Driven Catalytic Organic Synthesis. Journal of the American Chemical Society, 2016, 138, 6822-6828.	6.6	136
53	Insights into the excitonic processes in polymeric photocatalysts. Chemical Science, 2017, 8, 4087-4092.	3.7	136
54	A Unique Semiconductor–Metal–Graphene Stack Design to Harness Charge Flow for Photocatalysis. Advanced Materials, 2014, 26, 5689-5695	11.1	134

#	Article	IF	CITATIONS
55	Proliferation of Multidrug-Resistant New Delhi Metallo-β-lactamase Genes in Municipal Wastewater Treatment Plants in Northern China. Environmental Science and Technology Letters, 2014, 1, 26-30.	3.9	133
56	lonic Liquid Facilitates the Conjugative Transfer of Antibiotic Resistance Genes Mediated by Plasmid RP4. Environmental Science & Technology, 2015, 49, 8731-8740.	4.6	132
57	Heteroatom-assisted olefin polymerization by rare-earth metal catalysts. Science Advances, 2017, 3, e1701011.	4.7	122
58	Catalysed low temperature H2 release from nitrogen heterocycles. New Journal of Chemistry, 2006, 30, 1675.	1.4	121
59	Fate and proliferation of typical antibiotic resistance genes in five full-scale pharmaceutical wastewater treatment plants. Science of the Total Environment, 2015, 526, 366-373.	3.9	121
60	Insight into Electrocatalysts as Co-catalysts in Efficient Photocatalytic Hydrogen Evolution. ACS Catalysis, 2016, 6, 4253-4257.	5.5	120
61	Conjugative multi-resistant plasmids in Haihe River and their impacts on the abundance and spatial distribution of antibiotic resistance genes. Water Research, 2017, 111, 81-91.	5.3	114
62	Wide-bandgap organic–inorganic hybrid and all-inorganic perovskite solar cells and their application in all-perovskite tandem solar cells. Energy and Environmental Science, 2021, 14, 5723-5759.	15.6	114
63	Aggregation-enhanced luminescence and vibronic coupling of silole molecules from first principles. Physical Review B, 2006, 73, .	1.1	113
64	Unraveling the formation mechanism of graphitic nitrogen-doping in thermally treated graphene with ammonia. Scientific Reports, 2016, 6, 23495.	1.6	111
65	Single Crystalline Submicrotubes from Small Organic Molecules. Chemistry of Materials, 2005, 17, 6430-6435.	3.2	110
66	First-Principles Study on Transition-Metal Dichalcogenide/BSe van der Waals Heterostructures: A Promising Water-Splitting Photocatalyst. Journal of Physical Chemistry C, 2019, 123, 22742-22751.	1.5	110
67	High-efficiency photocatalyst for water splitting: a Janus MoSSe/XN (X  =  Ga, Al) van der Waals heterostructure. Journal Physics D: Applied Physics, 2020, 53, 185504.	1.3	110
68	Coherent Random Fiber Laser Based on Nanoparticles Scattering in the Extremely Weakly Scattering Regime. Physical Review Letters, 2012, 109, 253901.	2.9	108
69	Spatialâ€Temporal Variation of Lake Surface Water Temperature and Its Driving Factors in Yunnanâ€Guizhou Plateau. Water Resources Research, 2019, 55, 4688-4703.	1.7	108
70	Graphene–boron nitride hybrid-supported single Mo atom electrocatalysts for efficient nitrogen reduction reaction. Journal of Materials Chemistry A, 2019, 7, 15173-15180.	5.2	107
71	Computational Study of Titanocene-Catalyzed Dehydrocoupling of the Adduct Me2NH·BH3: An Intramolecular, Stepwise Mechanism. Organometallics, 2007, 26, 3597-3600.	1.1	106
72	Accurate Determination of Interfacial Protein Secondary Structure by Combining Interfacial-Sensitive Amide I and Amide III Spectral Signals. Journal of the American Chemical Society, 2014, 136, 1206-1209.	6.6	106

#	Article	IF	CITATIONS
73	Transition-metal dichalcogenides/Mg(OH) <sub>2</sub> van der Waals heterostructures as promising water-splitting photocatalysts: a first-principles study. Physical Chemistry Chemical Physics, 2019, 21, 1791-1796.	1.3	106
74	Ultrahigh Carrier Mobility in the Two-Dimensional Semiconductors B <sub>8</sub> Si <sub>4</sub> , B <sub>8</sub> Ge <sub>4</sub> , and B <sub>8</sub> Sn <sub>4</sub> . Chemistry of Materials, 2021, 33, 6475-6483.	3.2	104
75	Arctic antibiotic resistance gene contamination, a result of anthropogenic activities and natural origin. Science of the Total Environment, 2018, 621, 1176-1184.	3.9	102
76	Oxyhydroxide Nanosheets with Highly Efficient Electron–Hole Pair Separation for Hydrogen Evolution. Angewandte Chemie - International Edition, 2016, 55, 2137-2141.	7.2	99
77	Large two-photon absorption cross sections in two-dimensional, charge-transfer, cumulene-containing aromatic molecules. Journal of Chemical Physics, 1999, 111, 7758-7765.	1.2	98
78	The Microscopic Structure of Liquid Methanol from Raman Spectroscopy. Journal of Physical Chemistry B, 2010, 114, 3567-3573.	1.2	98
79	In situ Integration of a Metallic 1Tâ€MoS <sub>2</sub> /CdS Heterostructure as a Means to Promote Visibleâ€Lightâ€Driven Photocatalytic Hydrogen Evolution. ChemCatChem, 2016, 8, 2614-2619.	1.8	98
80	Narrowband Emission from Organic Fluorescent Emitters with Dominant Lowâ€Frequency Vibronic Coupling. Advanced Optical Materials, 2021, 9, 2001845.	3.6	98
81	Solvent effects on the electronic structure of a newly synthesized two-photon polymerization initiator. Journal of Chemical Physics, 2003, 119, 1208-1213.	1.2	97
82	A quantum chemistry approach for currentââ,¬â€œvoltage characterization of molecular junctions. Physical Chemistry Chemical Physics, 2001, 3, 5017-5023.	1.3	95
83	Lighting Up the Invisible Twisted Intramolecular Charge Transfer State by High Pressure. Journal of Physical Chemistry Letters, 2019, 10, 748-753.	2.1	95
84	Unusual Thiolate-Bridged Diiron Clusters Bearing the <i>cis</i> -HNâ•NH Ligand and Their Reactivities with Terminal Alkynes. Journal of the American Chemical Society, 2011, 133, 1147-1149.	6.6	94
85	A New Cubic Phase for a NaYF <sub>4</sub> Host Matrix Offering High Upconversion Luminescence Efficiency. Advanced Materials, 2015, 27, 5528-5533.	11.1	94
86	Role of the co-catalyst in the asymmetric coupling of racemic epoxides with CO2 using multichiral Co(iii) complexes: product selectivity and enantioselectivity. Chemical Science, 2012, 3, 2094.	3.7	93
87	Theoretical Modeling of Plasmon-Enhanced Raman Images of a Single Molecule with Subnanometer Resolution. Journal of the American Chemical Society, 2015, 137, 9515-9518.	6.6	92
88	Electrically driven single-photon emission from an isolated single molecule. Nature Communications, 2017, 8, 580.	5.8	92
89	Visually constructing the chemical structure of a single molecule by scanning Raman picoscopy. National Science Review, 2019, 6, 1169-1175.	4.6	91
90	Design and control of electron transport properties of single molecules. Proceedings of the National Academy of Sciences of the United States of America, 2009, 106, 15259-15263.	3.3	88

#	Article	IF	CITATIONS
91	Oxidation states of graphene: Insights from computational spectroscopy. Journal of Chemical Physics, 2009, 131, 244505.	1.2	88
92	Synergistic Effect of Surface-Terminated Oxygen Vacancy and Single-Atom Catalysts on Defective MXenes for Efficient Nitrogen Fixation. Journal of Physical Chemistry Letters, 2020, 11, 5051-5058.	2.1	88
93	First-Principles Simulations of Inelastic Electron Tunneling Spectroscopy of Molecular Electronic Devices. Nano Letters, 2005, 5, 1551-1555.	4.5	87
94	Chemical and electronic structures of liquid methanol from x-ray emission spectroscopy and density functional theory. Physical Review B, 2005, 71, .	1.1	87
95	What Are the Adsorption Sites for CO on the Reduced TiO <sub>2</sub> (110)-1 × 1 Surface?. Journal of the American Chemical Society, 2009, 131, 7958-7959.	6.6	87
96	ortho-Selective C–H addition of N,N-dimethyl anilines to alkenes by a yttrium catalyst. Chemical Science, 2016, 7, 5265-5270.	3.7	87
97	Non-catalytic hydrogenation of VO2 in acid solution. Nature Communications, 2018, 9, 818.	5.8	87
98	Heavy metal copper accelerates the conjugative transfer of antibiotic resistance genes in freshwater microcosms. Science of the Total Environment, 2020, 717, 137055.	3.9	87
99	Combining photocatalytic hydrogen generation and capsule storage in graphene based sandwich structures. Nature Communications, 2017, 8, 16049.	5.8	86
100	Strain-enhanced properties of van der Waals heterostructure based on blue phosphorus and g-GaN as a visible-light-driven photocatalyst for water splitting. RSC Advances, 2019, 9, 4816-4823.	1.7	86
101	Direct writing of electronic devices on graphene oxide by catalytic scanning probe lithography. Nature Communications, 2012, 3, 1194.	5.8	85
102	Organic field-effect optical waveguides. Nature Communications, 2018, 9, 4790.	5.8	85
103	Dinitrogen Activation by Dihydrogen and a PNP-Ligated Titanium Complex. Journal of the American Chemical Society, 2017, 139, 1818-1821.	6.6	83
104	Occurrence and distribution of clinical and veterinary antibiotics in the faeces of a Chinese population. Journal of Hazardous Materials, 2020, 383, 121129.	6.5	83
105	Active Sites of Pd-Doped Flat and Stepped Cu(111) Surfaces for H <sub>2</sub> Dissociation in Heterogeneous Catalytic Hydrogenation. ACS Catalysis, 2013, 3, 1245-1252.	5.5	79
106	X-ray absorption spectra of graphene from first-principles simulations. Physical Review B, 2010, 82, .	1.1	78
107	An Ionic Liquid Facilitates the Proliferation of Antibiotic Resistance Genes Mediated by Class I Integrons. Environmental Science and Technology Letters, 2014, 1, 266-270.	3.9	78
108	A van der Waals Heterostructure Based on Graphene-like Gallium Nitride and Boron Selenide: A High-Efficiency Photocatalyst for Water Splitting. ACS Omega, 2019, 4, 21689-21697.	1.6	78

#	Article	IF	CITATIONS
109	Catalytic Activity of Single Transition-Metal Atom Doped in Cu(111) Surface for Heterogeneous Hydrogenation. Journal of Physical Chemistry C, 2013, 117, 14618-14624.	1.5	77
110	Occurrence and reduction of antibiotic resistance genes in conventional and advanced drinking water treatment processes. Science of the Total Environment, 2019, 669, 777-784.	3.9	77
111	Determining structural and chemical heterogeneities of surface species at the single-bond limit. Science, 2021, 371, 818-822.	6.0	77
112	Unraveling the Mechanism for the Sharpâ€Tip Enhanced Electrocatalytic Carbon Dioxide Reduction: The Kinetics Decide. Angewandte Chemie - International Edition, 2017, 56, 15617-15621.	7.2	76
113	Thermally Activated Delayed Fluorescence in an Organic Cocrystal: Narrowing the Singlet–Triplet Energy Gap via Charge Transfer. Angewandte Chemie - International Edition, 2019, 58, 11311-11316.	7.2	76
114	Versatile Roomâ€Temperatureâ€Phosphorescent Materials Prepared from Nâ€Substituted Naphthalimides: Emission Enhancement and Chemical Conjugation. Angewandte Chemie, 2016, 128, 10026-10030.	1.6	75
115	Fabrication of Graphene Nanomesh and Improved Chemical Enhancement for Raman Spectroscopy. Journal of Physical Chemistry C, 2012, 116, 15741-15746.	1.5	74
116	Effects of dipole alignment and channel interference on two-photon absorption cross sections of two-dimensional charge-transfer systems. Journal of Chemical Physics, 2002, 117, 11102-11106.	1.2	73
117	Location of Trapped Hole on Rutile-TiO2(110) Surface and Its Role in Water Oxidation. Journal of Physical Chemistry C, 2012, 116, 7863-7866.	1.5	73
118	CeO <sub>2</sub> Nanoparticles Regulate the Propagation of Antibiotic Resistance Genes by Altering Cellular Contact and Plasmid Transfer. Environmental Science & Technology, 2020, 54, 10012-10021.	4.6	73
119	Towards high-performance sustainable polymers via isomerization-driven irreversible ring-opening polymerization of five-membered thionolactones. Nature Chemistry, 2022, 14, 294-303.	6.6	73
120	Bio–nano interaction of proteins adsorbed on single-walled carbon nanotubes. Carbon, 2009, 47, 967-973.	5.4	72
121	Analysis on driving factors of lake surface water temperature for major lakes in Yunnan-Guizhou Plateau. Water Research, 2020, 184, 116018.	5.3	72
122	Experimental Identification of Ultrafast Reverse Hole Transfer at the Interface of the Photoexcited Methanol/Graphitic Carbon Nitride System. Angewandte Chemie - International Edition, 2018, 57, 5320-5324.	7.2	71
123	Current–voltage characteristics of single molecular junction: Dimensionality of metal contacts. Journal of Chemical Physics, 2003, 119, 4923-4928.	1.2	70
124	Density functional theory study of vibronic structure of the first absorption Qx band in free-base porphin. Spectrochimica Acta - Part A: Molecular and Biomolecular Spectroscopy, 2006, 65, 308-323.	2.0	70
125	Scandium-Catalyzed Regio- and Stereoselective Cyclopolymerization of Functionalized α,ï‰-Dienes and Copolymerization with Ethylene. Journal of the American Chemical Society, 2019, 141, 12624-12633.	6.6	70
126	Municipal Solid Waste Treatment System Increases Ambient Airborne Bacteria and Antibiotic Resistance Genes. Environmental Science & Technology, 2020, 54, 3900-3908.	4.6	70

#	Article	IF	CITATIONS
127	Novel heterocycle-based organic molecules with two-photon induced blue fluorescent emission. Journal of Materials Chemistry, 2003, 13, 708-711.	6.7	68
128	Solvent effects on two-photon absorption of dialkylamino substituted distyrylbenzene chromophore. Journal of Chemical Physics, 2007, 126, 204509.	1.2	68
129	Two-photon excited hemoglobin fluorescence. Biomedical Optics Express, 2011, 2, 71. CO <mml:math <="" td="" xmlns:mml="http://www.w3.org/1998/Math/MathML"><td>1.5</td><td>68</td></mml:math>	1.5	68
130	display="inline"> <mml:msub> <mml:mrow /&gt; <mml:mn>2 </mml:mn> </mml:mrow </mml:msub> dissociation activated through electron attachment on the reduced rutile TiO <mml:math <br="" xmlns:mml="http://www.w3.org/1998/Math/MathML">display="inline"&gt; <mml:msub> <mml:mrow< td=""><td>1.1</td><td>68</td></mml:mrow<></mml:msub></mml:math>	1.1	68
131	/> <mml:mn>2</mml:mn> (110)-1 <mml:math mlns:mml_"http://www.w3.org/1998 Mechanistic Insights into Scandium-Catalyzed Hydroaminoalkylation of Olefins with Amines: Origin of Regioselectivity and Charge-Based Prediction Model. Organometallics, 2017, 36, 1557-1565.</mml:math 	1.1	67
132	Risk assessment of antibiotic resistance genes in the drinking water system. Science of the Total Environment, 2021, 800, 149650.	3.9	67
133	Mechanistic Investigation on Scandium-Catalyzed C–H Addition of Pyridines to Olefins. Organometallics, 2012, 31, 3930-3937.	1.1	66
134	Exposure to phthalates in patients with diabetes and its association with oxidative stress, adiponectin, and inflammatory cytokines. Environment International, 2017, 109, 53-63.	4.8	66
135	Using van der Waals heterostructures based on two-dimensional blue phosphorus and XC (X = Ge, Si) for water-splitting photocatalysis: a first-principles study. Physical Chemistry Chemical Physics, 2019, 21, 9949-9956.	1.3	66
136	Metal-Free Boron Nitride Nanoribbon Catalysts for Electrochemical CO <sub>2</sub> Reduction: Combining High Activity and Selectivity. ACS Applied Materials & Interfaces, 2019, 11, 906-915.	4.0	66
137	Making silole photovoltaically active by attaching carbazolyl donor groups to the silolyl acceptor core. Chemical Communications, 2005, , 3583.	2.2	65
138	Quantum Chemistry Study of H <sup>+</sup> (H <sub>2</sub> O) <sub>8</sub> :  A Global Search for Its Isomers by the Scaled Hypersphere Search Method, and Its Thermal Behavior. Journal of Physical Chemistry A, 2007, 111, 10732-10737.	1.1	65
139	Tunable Hydrogen Doping of Metal Oxide Semiconductors with Acid–Metal Treatment at Ambient Conditions. Journal of the American Chemical Society, 2020, 142, 4136-4140.	6.6	65
140	Electric Dipole Descriptor for Machine Learning Prediction of Catalyst Surface–Molecular Adsorbate Interactions. Journal of the American Chemical Society, 2020, 142, 7737-7743.	6.6	65
141	Solvent dependence of solvatochromic shifts and the first hyperpolarizability of para-nitroaniline: A nonmonotonic behavior. Journal of Chemical Physics, 2003, 119, 4409-4412.	1.2	64
142	Water-catalyzed gas-phase reaction of formic acid with hydroxyl radical: A computational investigation. Chemical Physics Letters, 2009, 469, 57-61.	1.2	64
143	The Realistic Domain Structure of As-Synthesized Graphene Oxide from Ultrafast Spectroscopy. Journal of the American Chemical Society, 2013, 135, 12468-12474.	6.6	64
144	Dehydrogenation of Propane to Propylene by a Pd/Cu Single-Atom Catalyst: Insight from First-Principles Calculations. Journal of Physical Chemistry C, 2015, 119, 1016-1023.	1.5	64

#	Article	IF	CITATIONS
145	A generalized quantum chemical approach for elastic and inelastic electron transports in molecular electronics devices. Journal of Chemical Physics, 2006, 124, 034708.	1.2	63
146	Antibiotic Resistance Gene-Carrying Plasmid Spreads into the Plant Endophytic Bacteria using Soil Bacteria as Carriers. Environmental Science & Technology, 2021, 55, 10462-10470.	4.6	63
147	Regulating Electronic Spin Moments of Single-Atom Catalyst Sites via Single-Atom Promoter Tuning on S-Vacancy MoS <sub>2</sub> for Efficient Nitrogen Fixation. Journal of Physical Chemistry Letters, 2021, 12, 8355-8362.	2.1	63
148	Electrically Driven Single-Photon Superradiance from Molecular Chains in a Plasmonic Nanocavity. Physical Review Letters, 2019, 122, 233901.	2.9	62
149	Observation of inhomogeneous plasmonic field distribution in a nanocavity. Nature Nanotechnology, 2020, 15, 922-926.	15.6	62
150	Evidence of van Hove Singularities in Ordered Grain Boundaries of Graphene. Physical Review Letters, 2014, 112, 226802.	2.9	61
151	QM/MM Studies on Scandium-Catalyzed Syndiospecific Copolymerization of Styrene and Ethylene. Organometallics, 2011, 30, 2908-2919.	1.1	60
152	Machine Learning Protocol for Surface-Enhanced Raman Spectroscopy. Journal of Physical Chemistry Letters, 2019, 10, 6026-6031.	2.1	60
153	Integrated Design of Organic Hole Transport Materials for Efficient Solidâ€State Dyeâ€Sensitized Solar Cells. Advanced Energy Materials, 2015, 5, 1401185.	10.2	59
154	Pd <sub>4</sub> S <sub>3</sub> Se <sub>3</sub> , Pd <sub>4</sub> S <sub>3</sub> Te <sub>3</sub> , and Pd <sub>4</sub> Se <sub>3</sub> Te <sub>3</sub> : Candidate Two-Dimensional Janus Materials for Photocatalytic Water Splitting. Chemistry of Materials, 2021, 33, 4128-4134.	3.2	59
155	Misfolding of a Human Islet Amyloid Polypeptide at the Lipid Membrane Populates through β-Sheet Conformers without Involving α-Helical Intermediates. Journal of the American Chemical Society, 2019, 141, 1941-1948.	6.6	58
156	Effects of Protonation, Hydrogen Bonding, and Photodamaging on X-ray Spectroscopy of the Amine Terminal Group in Aminothiolate Monolayers. Journal of Physical Chemistry C, 2012, 116, 12649-12654.	1.5	57
157	Homometallic Rareâ€Earth Metal Phosphinidene Clusters: Synthesis and Reactivity. Angewandte Chemie - International Edition, 2014, 53, 1053-1056.	7.2	57
158	Catalytic activity of Pd-doped Cu nanoparticles for hydrogenation as a single-atom-alloy catalyst. Physical Chemistry Chemical Physics, 2014, 16, 8367-8375.	1.3	57
159	Hydrogenâ€Đopingâ€Induced Metalâ€Like Ultrahigh Freeâ€Carrier Concentration in Metalâ€Oxide Material for Giant and Tunable Plasmon Resonance. Advanced Materials, 2020, 32, e2004059.	11.1	57
160	Nature of the Entire Range of Rare Earth Metal-Based Cationic Catalysts for Highly Active and Syndioselective Styrene Polymerization. ACS Catalysis, 2016, 6, 176-185.	5.5	56
161	Asymmetric photon transport in organic semiconductor nanowires through electrically controlled exciton diffusion. Science Advances, 2018, 4, eaap9861.	4.7	56
162	Antibiotic resistance genes attenuated with salt accumulation in saline soil. Journal of Hazardous Materials, 2019, 374, 35-42.	6.5	56

#	Article	IF	CITATIONS
163	CO <sub>2</sub> Activation by Lewis Pairs Generated Under Copper Catalysis Enables Difunctionalization of Imines. Journal of the American Chemical Society, 2020, 142, 1966-1974.	6.6	56
164	A MoSSe/blue phosphorene vdw heterostructure with energy conversion efficiency of 19.9% for photocatalytic water splitting. Semiconductor Science and Technology, 2020, 35, 125008.	1.0	56
165	A neural network protocol for electronic excitations of <i>N</i> -methylacetamide. Proceedings of the United States of America, 2019, 116, 11612-11617.	3.3	55
166	Transition metal doped puckered arsenene: Magnetic properties and potential as a catalyst. Physica E: Low-Dimensional Systems and Nanostructures, 2019, 108, 153-159.	1.3	55
167	Mechanism for the Extremely Efficient Sensitization of Yb <sup>3+</sup> Luminescence in CsPbCl <sub>3</sub> Nanocrystals. Journal of Physical Chemistry Letters, 2019, 10, 487-492.	2.1	55
168	Conformational disorder of organic cations tunes the charge carrier mobility in two-dimensional organic-inorganic perovskites. Nature Communications, 2020, 11, 5481.	5.8	55
169	Impact of Active Site Density on Oxygen Reduction Reactions Using Monodispersed Fe–N–C Single-Atom Catalysts. ACS Applied Materials & Interfaces, 2020, 12, 15271-15278.	4.0	55
170	Synthesis and Electrocatalytic Property of Diiron Hydride Complexes Derived from a Thiolate-Bridged Diiron Complex. Inorganic Chemistry, 2015, 54, 10243-10249.	1.9	54
171	Direct Experimental Measurement of Donation/Back-Donation in Unsaturated Hydrocarbon Bonding to Metals. Journal of the American Chemical Society, 2000, 122, 12310-12316.	6.6	52
172	Density-Matrix Approach for the Electroluminescence of Molecules in a Scanning Tunneling Microscope. Physical Review Letters, 2011, 106, 177401.	2.9	52
173	Big Bandgap in Highly Reduced Graphene Oxides. Journal of Physical Chemistry C, 2013, 117, 6049-6054.	1.5	52
174	Lightâ€Induced Bidirectional Metalâ€toâ€Metal Charge Transfer in a Linear Fe <sub>2</sub> Co Complex. Angewandte Chemie - International Edition, 2017, 56, 7663-7668.	7.2	52
175	Gut microbiota exaggerates triclosan-induced liver injury via gut-liver axis. Journal of Hazardous Materials, 2022, 421, 126707.	6.5	52
176	Distinguishing Individual DNA Bases in a Network by Nonâ€Resonant Tipâ€Enhanced Raman Scattering. Angewandte Chemie - International Edition, 2017, 56, 5561-5564.	7.2	51
177	Investigation of Charge-Transfer Interaction in Mixed Stack Donor–Acceptor Cocrystals Toward Tunable Solid-State Emission Characteristics. Crystal Growth and Design, 2018, 18, 6001-6008.	1.4	51
178	Impact of urban expansion on vegetation: The case of China (2000–2018). Journal of Environmental Management, 2021, 291, 112598.	3.8	51
179	Increased chemical enhancement of Raman spectra for molecules adsorbed on fluorinated reduced graphene oxide. Carbon, 2012, 50, 4512-4517.	5.4	50
180	Hybrid Interface States and Spin Polarization at Ferromagnetic Metal–Organic Heterojunctions: Interface Engineering for Efficient Spin Injection in Organic Spintronics. Advanced Functional Materials, 2014, 24, 4812-4821.	7.8	50

#	Article	IF	CITATIONS
181	Mechanistic Insights into Ring Cleavage and Contraction of Benzene over a Titanium Hydride Cluster. Journal of the American Chemical Society, 2016, 138, 11550-11559.	6.6	50
182	Prevalence and Fate of Carbapenemase Genes in a Wastewater Treatment Plant in Northern China. PLoS ONE, 2016, 11, e0156383.	1.1	50
183	Theory for Vibrationally Resolved Two-Photon Circular Dichroism Spectra. Application to (R)-(+)-3-Methylcyclopentanone. Journal of Physical Chemistry A, 2009, 113, 4198-4207.	1.1	49
184	Design of Graphene-Nanoribbon Heterojunctions from First Principles. Journal of Physical Chemistry C, 2011, 115, 12616-12624.	1.5	49
185	Charge transfer and retention in directly coupled Au-CdSe nanohybrids. Nano Research, 2012, 5, 88-98.	5.8	49
186	A highly efficient and tumor vascular-targeting therapeutic technique with size-expansible gadofullerene nanocrystals. Science China Materials, 2015, 58, 799-810.	3.5	49
187	Fate and removal of various antibiotic resistance genes in typical pharmaceutical wastewater treatment systems. Environmental Science and Pollution Research, 2016, 23, 12030-12038.	2.7	49
188	Cooperative Trimerization of Carbon Monoxide by Lithium and Samarium Boryls. Journal of the American Chemical Society, 2017, 139, 16967-16973.	6.6	49
189	Hydrogen bonding effects on infrared and Raman spectra of drug molecules. Spectrochimica Acta - Part A: Molecular and Biomolecular Spectroscopy, 2007, 66, 213-224.	2.0	48
190	A first-principles study of NO adsorption and oxidation on Au(111) surface. Journal of Chemical Physics, 2008, 129, 134708.	1.2	48
191	Ultrafast Vibrational Dynamics of Membraneâ€Bound Peptides at the Lipid Bilayer/Water Interface. Angewandte Chemie - International Edition, 2017, 56, 12977-12981.	7.2	48
192	Acid-Promoted D-A-D Type Far-Red Fluorescent Probe with High Photostability for Lysosomal Nitric Oxide Imaging. Analytical Chemistry, 2018, 90, 7953-7962.	3.2	48
193	Vibronically-induced change in the chiral response of molecules revealed by electronic circular dichroism spectroscopy. Chemical Physics Letters, 2008, 464, 144-149.	1.2	47
194	Inelastic Electron Tunneling Spectroscopy of Goldâ^'Benzenedithiolâ^'Gold Junctions: Accurate Determination of Molecular Conformation. ACS Nano, 2011, 5, 2257-2263.	7.3	47
195	Vibrationally resolved high-resolution NEXAFS and XPS spectra of phenanthrene and coronene. Journal of Chemical Physics, 2014, 141, 044313.	1.2	47
196	B(C <sub>6</sub> F <sub>5</sub> ) <sub>3</sub> /Amine atalyzed C(sp)â^'H Silylation of Terminal Alkynes with Hydrosilanes: Experimental and Theoretical Studies. Angewandte Chemie - International Edition, 2018, 57, 15222-15226.	7.2	47
197	Predictions of Novel Two-Photon Absorption Bands in Fluorescent Proteins. Journal of Physical Chemistry B, 2007, 111, 14043-14050.	1.2	46
198	Visualization of Vibrational Modes in Real Space by Tipâ€Enhanced Nonâ€Resonant Raman Spectroscopy. Angewandte Chemie - International Edition, 2016, 55, 1041-1045.	7.2	46

#	Article	IF	CITATIONS
199	Hydrodenitrogenation of pyridines and quinolines at a multinuclear titanium hydride framework. Nature Communications, 2017, 8, 1866.	5.8	46
200	Photolysis mechanism of sulfonamide moiety in five-membered sulfonamides: A DFT study. Chemosphere, 2018, 197, 569-575.	4.2	46
201	One-Pot Synthesis of Diblock Polyesters by Catalytic Terpolymerization of Lactide, Epoxides, and Anhydrides. Macromolecules, 2019, 52, 3462-3470.	2.2	46
202	Identification of Alcohol Conformers by Raman Spectra in the C–H Stretching Region. Journal of Physical Chemistry A, 2015, 119, 3209-3217.	1.1	45
203	Experimental and Computational Studies of Dinitrogen Activation and Hydrogenation at a Tetranuclear Titanium Imide/Hydride Framework. Journal of the American Chemical Society, 2019, 141, 2713-2720.	6.6	45
204	Regiodivergent C–H Alkylation of Quinolines with Alkenes by Half-Sandwich Rare-Earth Catalysts. Journal of the American Chemical Society, 2020, 142, 18128-18137.	6.6	45
205	Surface Landau levels and spin states in bismuth (111) ultrathin films. Nature Communications, 2016, 7, 10814.	5.8	45
206	Automated exploration of stable isomers of H <sup>+</sup> (H <sub>2</sub> O) <i><sub>n</sub></i> ( <i>n</i> = 5–7) via <i>ab initio</i> calculations: An application of the anharmonic downward distortion following algorithm. Journal of Computational Chemistry, 2009, 30, 952-961.	1.5	44
207	Reorientation dynamics in liquid alcohols from Raman spectroscopy. Journal of Raman Spectroscopy, 2012, 43, 82-88.	1.2	44
208	Discharge of KPC-2 genes from the WWTPs contributed to their enriched abundance in the receiving river. Science of the Total Environment, 2017, 581-582, 136-143.	3.9	44
209	Single nickel atom supported on hybridized graphene–boron nitride nanosheet as a highly active bi-functional electrocatalyst for hydrogen and oxygen evolution reactions. Journal of Materials Chemistry A, 2019, 7, 26261-26265.	5.2	44
210	A Hydrogenated Metal Oxide with Full Solar Spectrum Absorption for Highly Efficient Photothermal Water Evaporation. Journal of Physical Chemistry Letters, 2020, 11, 2502-2509.	2.1	44
211	Temperature-Dependent Statistical Behavior of Single Molecular Conductance in Aqueous Solution. Journal of the American Chemical Society, 2008, 130, 6674-6675.	6.6	43
212	Simultaneous Analysis of Selected Typical Antibiotics in Manure by Microwave-Assisted Extraction and LC–MS n. Chromatographia, 2010, 71, 217-223.	0.7	43
213	Unprecedented 3,4-Isoprene and <i>cis</i> -1,4-Butadiene Copolymers with Controlled Sequence Distribution by Single Yttrium Cationic Species. Macromolecules, 2014, 47, 8524-8530.	2.2	43
214	Reorganization of hydrogen bond network makes strong polyelectrolyte brushes pH-responsive. Science Advances, 2016, 2, e1600579.	4.7	43
215	Ketones as Molecular Co atalysts for Boosting Excitonâ€Based Photocatalytic Molecular Oxygen Activation. Angewandte Chemie - International Edition, 2020, 59, 11093-11100.	7.2	43
216	Modeling of dynamic molecular solvent properties using local and cavity field approaches. Journal of Chemical Physics, 2000, 112, 1868-1875.	1.2	42

#	Article	IF	CITATIONS
217	Occurrence and Distribution of Urban Dust-Associated Bacterial Antibiotic Resistance in Northern China. Environmental Science and Technology Letters, 2018, 5, 50-55.	3.9	42
218	Influence of electron-acceptor strength on the resonant two-photon absorption cross sections of diphenylaminofluorene-based chromophores. Physical Chemistry Chemical Physics, 2003, 5, 3869-3873.	1.3	41
219	Basis set dependence of the doubly hybrid XYG3 functional. Journal of Chemical Physics, 2010, 133, 104105.	1.2	41
220	Computational Studies on Isospecific Polymerization of 1-Hexene Catalyzed by Cationic Rare Earth Metal Alkyl Complex Bearing a <i>C</i> <sub>3</sub> <i>i</i> Pr-trisox Ligand. Macromolecules, 2012, 45, 640-651.	2.2	41
221	GGA+U Study on the Mechanism of Photodecomposition of Water Adsorbed on Rutile TiO <sub>2</sub> (110) Surface: Free vs Trapped Hole. Journal of Physical Chemistry C, 2014, 118, 1027-1034.	1.5	41
222	Theoretical Mechanistic Studies on the <i>trans</i> -1,4-Specific Polymerization of Isoprene Catalyzed by a Cationic La–Al Binuclear Complex. Macromolecules, 2014, 47, 4596-4606.	2.2	41
223	DFT Studies on the Silver-Catalyzed Carboxylation of Terminal Alkynes with CO <sub>2</sub> : An Insight into the Catalytically Active Species. Organometallics, 2014, 33, 2984-2989.	1.1	41
224	Ultrafast energy relaxation dynamics of amide I vibrations coupled with protein-bound water molecules. Nature Communications, 2019, 10, 1010.	5.8	41
225	A time-series analysis of urbanization-induced impervious surface area extent in the Dianchi Lake watershed from 1988–2017. International Journal of Remote Sensing, 2019, 40, 573-592.	1.3	41
226	Alkali Metal Carboxylates: Simple and Versatile Initiators for Ring-Opening Alternating Copolymerization of Cyclic Anhydrides/Epoxides. Macromolecules, 2021, 54, 713-724.	2.2	41
227	Direct copolymerization of ethylene with protic comonomers enabled by multinuclear Ni catalysts. Nature Communications, 2021, 12, 6283.	5.8	41
228	Hybrid density-functional theory calculations of near-edge x-ray absorption fine-structure spectra: Applications on benzonitrile in gas phase. Physical Review A, 2005, 71, .	1.0	40
229	Probing Moleculeâ^'Metal Bonding in Molecular Junctions by Inelastic Electron Tunneling Spectroscopy. Nano Letters, 2006, 6, 1693-1698.	4.5	40
230	XYG3s: Speedup of the XYG3 fifth-rung density functional with scaling-all-correlation method. Journal of Chemical Physics, 2010, 132, 194105.	1.2	40
231	The Raman enhancement effect on a thin GaSe flake and its thickness dependence. Journal of Materials Chemistry C, 2015, 3, 11129-11134.	2.7	40
232	Gut resistomes, microbiota and antibiotic residues in Chinese patients undergoing antibiotic administration and healthy individuals. Science of the Total Environment, 2020, 705, 135674.	3.9	40
233	Toward Rational Design of Dual-Metal-Site Catalysts: Catalytic Descriptor Exploration. ACS Catalysis, 2022, 12, 3420-3429.	5.5	40
234	The structural determination of endohedral metallofullerene Gd@C <sub>82</sub> by XANES. Chemical Communications, 2008, , 474-476.	2.2	39

#	Article	IF	CITATIONS
235	Trends in Râ^'X Bond Dissociation Energies (R• = Me, Et, i-Pr, t-Bu, X• = H, Me, Cl, OH). Journal of Chemical Theory and Computation, 2010, 6, 1462-1469.	2.3	39
236	Electroluminescence of molecules in a scanning tunneling microscope: Role of tunneling electrons and surface plasmons. Physical Review B, 2011, 84, .	1.1	39
237	Dinitrogen Activation and Hydrogenation by C <sub>5</sub> Me <sub>4</sub> SiMe <sub>3</sub> -Ligated Di- and Trinuclear Chromium Hydride Complexes. Journal of the American Chemical Society, 2020, 142, 9007-9016.	6.6	39
238	EPR detection of hydroxyl radical generation and its interaction with antioxidant system in Carassius auratus exposed to pentachlorophenol. Journal of Hazardous Materials, 2009, 171, 1096-1102.	6.5	38
239	First-Principles Study of Electrochemical Gate-Controlled Conductance in Molecular Junctions. Nano Letters, 2006, 6, 2091-2094.	4.5	37
240	Mechanistic Insights into the Copper-Cocatalyzed Sonogashira Cross-Coupling Reaction: Key Role of an Anion. Organometallics, 2017, 36, 1042-1048.	1.1	37
241	Direct Functionalization of White Phosphorus to Cyclotetraphosphanes: Selective Formation of Four P–C Bonds. Journal of the American Chemical Society, 2019, 141, 6843-6847.	6.6	37
242	Spatial–temporal variations in urbanization in Kunming and their impact on urban lake water quality. Land Degradation and Development, 2020, 31, 1392-1407.	1.8	37
243	Enantioselective Cyanoborylation of Allenes by <i>N</i> -Heterocyclic Carbene-Copper Catalysts. ACS Catalysis, 2020, 10, 11685-11692.	5.5	37
244	First Principles Study on the Geometric and Electronic Structures of the FeO/Pt(111) Surface. Journal of Physical Chemistry C, 2009, 113, 8302-8305.	1.5	36
245	Thermal assisted ultrasonic bonding method for poly(methyl methacrylate) (PMMA) microfluidic devices. Talanta, 2010, 81, 1331-1338.	2.9	36
246	Propagation of New Delhi Metallo-β-lactamase Genes ( <i>bla</i> <sub>NDM-1</sub> ) from a Wastewater Treatment Plant to Its Receiving River. Environmental Science and Technology Letters, 2016, 3, 138-143.	3.9	36
247	An NHC–Silyl–NHC Pincer Ligand for the Oxidative Addition of Câ^'H, Nâ^'H, and Oâ^'H Bonds to Cobalt(I) Complexes. Angewandte Chemie - International Edition, 2017, 56, 2720-2724.	7.2	36
248	First-principles calculations of aluminium nitride monolayer with chemical functionalization. Applied Surface Science, 2019, 481, 1549-1553.	3.1	36
249	Two-Photon Absorption of Hydrogen-Bonded Octupolar Molecule Clusters. Journal of Physical Chemistry B, 2008, 112, 4387-4392.	1.2	35
250	Plasmon resonances in linear noble-metal chains. Journal of Chemical Physics, 2012, 137, 194307.	1.2	35
251	Enhanced Activity of C <sub>2</sub> N-Supported Single Co Atom Catalyst by Single Atom Promoter. Journal of Physical Chemistry Letters, 2019, 10, 7009-7014.	2.1	35
252	Vibronic induced one- and two-photon absorption in a charge-transfer stilbene derivate. Journal of Chemical Physics, 2007, 126, 244509.	1.2	34

#	Article	IF	CITATIONS
253	In Situ Molecular-Level Insights into the Interfacial Structure Changes of Membrane-Associated Prion Protein Fragment [118–135] Investigated by Sum Frequency Generation Vibrational Spectroscopy. Langmuir, 2012, 28, 16979-16988.	1.6	34
254	Improving the photovoltaic performance of solid-state ZnO/CdTe core–shell nanorod array solar cells using a thin CdS interfacial layer. Journal of Materials Chemistry A, 2014, 2, 5675-5681.	5.2	34
255	Chiral and Regenerable NAD(P)H Models Enabled Biomimetic Asymmetric Reduction: Design, Synthesis, Scope, and Mechanistic Studies. Journal of Organic Chemistry, 2020, 85, 2355-2368.	1.7	34
256	Probing intramolecular vibronic coupling through vibronic-state imaging. Nature Communications, 2021, 12, 1280.	5.8	34
257	2-chlorophenol induced hydroxyl radical production in mitochondria in Carassius auratus and oxidative stress – An electron paramagnetic resonance study. Chemosphere, 2008, 71, 1260-1268.	4.2	33
258	Theoretical insights into the charge transport in perylene diimides based n-type organic semiconductors. Organic Electronics, 2012, 13, 2763-2772.	1.4	33
259	Phosphate Ions Promoting Association between Peptide and Modeling Cell Membrane Revealed by Sum Frequency Generation Vibrational Spectroscopy. Journal of Physical Chemistry C, 2013, 117, 11095-11103.	1.5	33
260	Roles of Plasmonic Excitation and Protonation on Photoreactions of <i>p</i> -Aminobenzenethiol on Ag Nanoparticles. Journal of Physical Chemistry C, 2014, 118, 6893-6902.	1.5	33
261	Airborne bacterial contaminations in typical Chinese wet market with live poultry trade. Science of the Total Environment, 2016, 572, 681-687.	3.9	33
262	Protecting Single Atom Catalysts with Graphene/Carbon-Nitride "Chainmail― Journal of Physical Chemistry Letters, 2019, 10, 3129-3133.	2.1	33
263	Exceeding the volcano relationship in oxygen reduction/evolution reactions using single-atom-based catalysts with dual-active-sites. Journal of Materials Chemistry A, 2020, 8, 10193-10198.	5.2	33
264	A Comparative Theoretical Study of Proton-Coupled Hole Transfer for H2O and Small Organic Molecules (CH3OH, HCOOH, H2CO) on the Anatase TiO2(101) Surface. Journal of Physical Chemistry C, 2014, 118, 21457-21462.	1.5	32
265	Half-filled energy bands induced negative differential resistance in nitrogen-doped graphene. Nanoscale, 2015, 7, 4156-4162.	2.8	32
266	Isomer-Specific Transplacental Efficiencies of Perfluoroalkyl Substances in Human Whole Blood. Environmental Science and Technology Letters, 2017, 4, 391-398.	3.9	32
267	Isolating hydrogen from oxygen in photocatalytic water splitting with a carbon-quantum-dot/carbon-nitride hybrid. Journal of Materials Chemistry A, 2019, 7, 6143-6148.	5.2	32
268	General theory for pulse propagation in two-photon active media. Journal of Chemical Physics, 2002, 117, 6214-6220.	1.2	31
269	Electronic Structure of Nitrogen-Doped Graphene in the Ground and Core-Excited States from First-Principles Simulations. Journal of Physical Chemistry C, 2015, 119, 16660-16666.	1.5	31
270	Protonation-Induced Room-Temperature Phosphorescence in Fluorescent Polyurethane. Journal of Physical Chemistry A, 2017, 121, 4225-4232.	1.1	31

#	Article	IF	CITATIONS
271	Visible Light-Induced Aerobic Epoxidation of α,β-Unsaturated Ketones Mediated by Amidines. Journal of Organic Chemistry, 2018, 83, 13051-13062.	1.7	31
272	Mixed Starter Culture Regulates Biogenic Amines Formation via Decarboxylation and Transamination during Chinese Rice Wine Fermentation. Journal of Agricultural and Food Chemistry, 2018, 66, 6348-6356.	2.4	31
273	Interfacial Hydrogen-Bonding Dynamics in Surface-Facilitated Dehydrogenation of Water on TiO <sub>2</sub> (110). Journal of the American Chemical Society, 2020, 142, 826-834.	6.6	31
274	Solvent effects on the polarizabilities and hyperpolarizabilities of conjugated polymers. Journal of Chemical Physics, 1999, 111, 9853-9858.	1.2	30
275	Electronic structures of azafullerene C48N12. Journal of Chemical Physics, 2003, 119, 7139-7144.	1.2	30
276	Quantum molecular dynamics study of water on TiO2(110) surface. Journal of Chemical Physics, 2008, 129, 064703.	1.2	30
277	Blinking, Flickering, and Correlation in Fluorescence of Single Colloidal CdSe Quantum Dots with Different Shells under Different Excitations. Journal of Physical Chemistry C, 2013, 117, 4844-4851.	1.5	30
278	Pressure-Induced Tunable Electron Transfer and Auger Recombination Rates in CdSe/ZnS Quantum Dot–Anthraquinone Complexes. Journal of Physical Chemistry Letters, 2019, 10, 3064-3070.	2.1	30
279	Vancomycin exposure caused opportunistic pathogens bloom in intestinal microbiome by simulator of the human intestinal microbial ecosystem (SHIME). Environmental Pollution, 2020, 265, 114399.	3.7	30
280	Ordered Water Layer on the Macroscopically Hydrophobic Fluorinated Polymer Surface and Its Ultrafast Vibrational Dynamics. Journal of the American Chemical Society, 2021, 143, 13074-13081.	6.6	30
281	Origin of the Q-band splitting in the absorption spectra of aluminum phthalocyanine chloride. Chemical Physics Letters, 2007, 438, 36-40.	1.2	29
282	First Principles Study of O <sub>2</sub> Adsorption on Reduced Rutile TiO <sub>2</sub> -(110) Surface Under UV Illumination and Its Role on CO Oxidation. Journal of Physical Chemistry C, 2013, 117, 956-961.	1.5	29
283	The horizontal transfer of antibiotic resistance genes is enhanced by ionic liquid with different structure of varying alkyl chain length. Frontiers in Microbiology, 2015, 6, 864.	1.5	29
284	Visible-Light Photoexcited Electron Dynamics of Scandium Endohedral Metallofullerenes: The Cage Symmetry and Substituent Effects. Journal of the American Chemical Society, 2015, 137, 8769-8774.	6.6	29
285	Role of the cavity field in nonlinear optical response in the condensed phase. Journal of Chemical Physics, 2001, 114, 3105-3108.	1.2	28
286	Molecular structure in water and solutions studied by photon-in/photon-out soft X-ray spectroscopy. Journal of Electron Spectroscopy and Related Phenomena, 2010, 177, 181-191.	0.8	28
287	Tuning Magnetism in Transition-Metal-Doped 3 <i>C</i> Silicon Carbide Polytype. Journal of Physical Chemistry C, 2011, 115, 253-256.	1.5	28
288	A density functional theory approach to mushroom-like platinum clusters on palladium-shell over Au core nanoparticles for high electrocatalytic activity. Physical Chemistry Chemical Physics, 2011, 13, 5441.	1.3	28

#	Article	IF	CITATIONS
289	DFT Studies on the Reduction of Dinitrogen to Ammonia by a Thiolate-Bridged Diiron Complex as a Nitrogenase Mimic. Organometallics, 2012, 31, 335-344.	1.1	28
290	In Situ and Real-Time SFG Measurements Revealing Organization and Transport of Cholesterol Analogue 6-Ketocholestanol in a Cell Membrane. Journal of Physical Chemistry Letters, 2014, 5, 419-424.	2.1	28
291	DFT Studies on Styrene Polymerization Catalyzed by Cationic Rare-Earth-Metal Complexes: Origin of Ligand-Dependent Activities. Organometallics, 2016, 35, 3205-3214.	1.1	28
292	Intermetallic Cooperation in Olefin Polymerization Catalyzed by a Binuclear Samarocene Hydride: A Theoretical Study. Organometallics, 2016, 35, 778-784.	1.1	28
293	Perfluoroalkyl Acids Including Isomers in Tree Barks from a Chinese Fluorochemical Manufacturing Park: Implication for Airborne Transportation. Environmental Science & Technology, 2018, 52, 2016-2024.	4.6	28
294	Molecular understanding of the interaction of amino acids with sulfuric acid in the presence of water and the atmospheric implication. Chemosphere, 2018, 210, 215-223.	4.2	28
295	Catalytic Chemistry Predicted by a Charge Polarization Descriptor: Synergistic O <sub>2</sub> Activation and CO Oxidation by Au–Cu Bimetallic Clusters on TiO <sub>2</sub> (101). ACS Applied Materials & Interfaces, 2019, 11, 9629-9640.	4.0	28
296	The prevalence of ampicillin-resistant opportunistic pathogenic bacteria undergoing selective stress of heavy metal pollutants in the Xiangjiang River, China. Environmental Pollution, 2021, 268, 115362.	3.7	28
297	Antibiotic contamination amplifies the impact of foreign antibiotic-resistant bacteria on soil bacterial community. Science of the Total Environment, 2021, 758, 143693.	3.9	28
298	Spectral identification of fullerene C82 isomers. Journal of Chemical Physics, 2007, 127, 164314.	1.2	27
299	Effect of Sulfate-Reducing Bacteria and Iron-Oxidizing Bacteria on the Rate of Corrosion of an Aluminum Alloy in a Central Air-Conditioning Cooling Water System. Industrial & Engineering Chemistry Research, 2014, 53, 7840-7846.	1.8	27
300	Computational Analyses of the Effect of Lewis Bases on Styrene Polymerization Catalyzed by Cationic Scandium Half-Sandwich Complexes. Organometallics, 2015, 34, 5540-5548.	1.1	27
301	A Secondâ€Coordinationâ€Sphere Strategy to Modulate Nickel―and Palladiumâ€Catalyzed Olefin Polymerization and Copolymerization. Angewandte Chemie, 2017, 129, 11762-11767.	1.6	27
302	Combining High Photocatalytic Activity and Stability via Subsurface Defects in TiO <sub>2</sub> . Journal of Physical Chemistry C, 2018, 122, 17221-17227.	1.5	27
303	Computational Investigation of Scandium-Based Catalysts for Olefin Hydroaminoalkylation and C–H Addition. Organometallics, 2019, 38, 1887-1896.	1.1	27
304	Accurate bond dissociation enthalpies by using doubly hybrid XYG3 functional. Journal of Computational Chemistry, 2011, 32, 1824-1838.	1.5	26
305	Oxyhydroxide Nanosheets with Highly Efficient Electron–Hole Pair Separation for Hydrogen Evolution. Angewandte Chemie, 2016, 128, 2177-2181.	1.6	26
306	Probing the ultrafast dynamics in nanomaterial complex systems by femtosecond transient absorption spectroscopy. High Power Laser Science and Engineering, 2016, 4, .	2.0	26

#	Article	IF	CITATIONS
307	Hollow Iron–Vanadium Composite Spheres: A Highly Efficient Ironâ€Based Water Oxidation Electrocatalyst without the Need for Nickel or Cobalt. Angewandte Chemie, 2017, 129, 3337-3341.	1.6	26
308	Spatiotemporal profile of tetracycline and sulfonamide and their resistance on a catchment scale. Environmental Pollution, 2018, 241, 1098-1105.	3.7	26
309	An elongation method for first principle simulations of electronic structures and electron transport properties of finite nanostructures. Journal of Chemical Physics, 2006, 124, 214711.	1.2	25
310	Refinement of DNA Structures through Near-Edge X-ray Absorption Fine Structure Analysis: Applications on Guanine and Cytosine Nucleobases, Nucleosides, and Nucleotides. Journal of Physical Chemistry B, 2010, 114, 13214-13222.	1.2	25
311	Diphosphazane-monoxide and Phosphine-sulfonate Palladium Catalyzed Ethylene Copolymerization with Polar Monomers: A Computational Study. Organometallics, 2019, 38, 638-646.	1.1	25
312	Cooperative Single-Atom Active Centers for Attenuating the Linear Scaling Effect in the Nitrogen Reduction Reaction. Journal of Physical Chemistry Letters, 2021, 12, 5233-5240.	2.1	25
313	Origin of the Anomalous Two-Photon Absorption in Fluorescent Protein DsRed. Journal of Physical Chemistry B, 2007, 111, 505-507.	1.2	24
314	Theoretical Studies on Photoisomerizations of (6â^'4) and Dewar Photolesions in DNA. Journal of Physical Chemistry B, 2010, 114, 14096-14102.	1.2	24
315	Systematic Study of Soft X-ray Spectra of Poly(Dg)·Poly(Dc) and Poly(Da)·Poly(Dt) DNA Duplexes. Journal of Physical Chemistry B, 2010, 114, 7016-7021.	1.2	24
316	Reversible Modification of CdSe–CdS/ZnS Quantum Dot Fluorescence by Surrounding Ca <sup>2+</sup> lons. Journal of Physical Chemistry C, 2014, 118, 10424-10433.	1.5	24
317	First-Principles Study on the Mechanism of Photoselective Catalytic Reduction of NO by NH <sub>3</sub> on Anatase TiO <sub>2</sub> (101) Surface. Journal of Physical Chemistry C, 2014, 118, 6359-6364.	1.5	24
318	Theory for Modeling of High Resolution Resonant and Nonresonant Raman Images. Journal of Chemical Theory and Computation, 2016, 12, 4986-4995.	2.3	24
319	Graphene Oxide-Supported Transition Metal Catalysts for Di-Nitrogen Reduction. Journal of Physical Chemistry C, 2018, 122, 25441-25446.	1.5	24
320	A combinatory approach towards the design of organic polymer luminescent materials. Journal of Materials Chemistry C, 2019, 7, 9917-9925.	2.7	24
321	Human activities and the natural environment have induced changes in the PM2.5 concentrations in Yunnan Province, China, over the past 19 years. Environmental Pollution, 2020, 265, 114878.	3.7	24
322	Chirality and diameter dependent x-ray absorption of single walled carbon nanotubes. Journal of Chemical Physics, 2009, 131, 034704.	1.2	23
323	Effect of Aromatic Coupling on Electronic Transport in Bimolecular Junctions. Journal of Physical Chemistry C, 2009, 113, 14474-14477.	1.5	23
324	First-Principles Study on Core-Level Spectroscopy of Arginine in Gas and Solid Phases. Journal of Physical Chemistry B, 2012, 116, 12641-12650.	1.2	23

#	Article	lF	CITATIONS
325	Theoretical Study of Core Excitations of Fullerene-Based Polymer Solar Cell Acceptors. Journal of Physical Chemistry C, 2012, 116, 23938-23944.	1.5	23
326	Intermolecular Interactions at the Interface Quantified by Surface-Sensitive Second-Order Fermi Resonant Signals. Journal of Physical Chemistry C, 2015, 119, 16587-16595.	1.5	23
327	Nonlinear bandgap opening behavior of BN co-doped graphene. Carbon, 2016, 107, 857-864.	5.4	23
328	Alkyl Effects on the Chain Initiation Efficiency of Olefin Polymerization by Cationic Half-Sandwich Scandium Catalysts: A DFT Study. Organometallics, 2016, 35, 913-920.	1.1	23
329	Isolation, structure and reactivity of a scandium boryl oxycarbene complex. Chemical Science, 2016, 7, 803-809.	3.7	23
330	The degradation mechanism of sulfamethoxazole under ozonation: a DFT study. Environmental Sciences: Processes and Impacts, 2017, 19, 379-387.	1.7	23
331	A Highly Sensitive Femtosecond Time-Resolved Sum Frequency Generation Vibrational Spectroscopy System with Simultaneous Measurement of Multiple Polarization Combinations. Chinese Journal of Chemical Physics, 2017, 30, 671-677.	0.6	23
332	Effective treatment of TNFα inhibitors in Chinese patients with Blau syndrome. Arthritis Research and Therapy, 2019, 21, 236.	1.6	23
333	First-principles investigation on electronic properties and band alignment of group III monochalcogenides. Scientific Reports, 2019, 9, 13289.	1.6	23
334	Theoretical insight into the redox-switchable activity of group 4 metal complexes for the ring-opening polymerization of ε-caprolactone. Inorganic Chemistry Frontiers, 2020, 7, 961-971.	3.0	23
335	Cooperative Nitrogen Activation and Ammonia Synthesis on Densely Monodispersed Mo–N–C Sites. Journal of Physical Chemistry Letters, 2020, 11, 3962-3968.	2.1	23
336	The prolonged disruption of a single-course amoxicillin on mice gut microbiota and resistome, and recovery by inulin, Bifidobacterium longum and fecal microbiota transplantation. Environmental Pollution, 2020, 265, 114651.	3.7	23
337	Structure dependent quantum confinement effect in hydrogen-terminated nanodiamond clusters. Journal of Applied Physics, 2010, 108, 094303.	1.1	22
338	A First Principles Study on the Dissociation and Rotation Processes of a Single O <sub>2</sub> Molecule on the Pt(111) Surface. Journal of Physical Chemistry C, 2011, 115, 6864-6869.	1.5	22
339	Differences in Twoâ€Photon and Oneâ€Photon Absorption Profiles Induced by Vibronic Coupling: The Case of Dioxaborine Heterocyclic Dye. ChemPhysChem, 2011, 12, 3392-3403.	1.0	22
340	X-ray spectroscopy of blocked alanine in water solution from supermolecular and supermolecular-continuum solvation models: a first-principles study. Physical Chemistry Chemical Physics, 2012, 14, 9666.	1.3	22
341	Direct nucleophilic trifluoromethylation using fluoroform: a theoretical mechanistic investigation and insight into the effect of alkali metal cations. New Journal of Chemistry, 2013, 37, 3274.	1.4	22
342	Density functional theory study on the adsorption and decomposition of the formic acid catalyzed by highly active mushroom-like Au@Pd@Pt tri-metallic nanoparticles. Physical Chemistry Chemical Physics, 2013, 15, 4625.	1.3	22

#	Article	IF	CITATIONS
343	Fluorescence and Phosphorescence of Single C <sub>60</sub> Molecules as Stimulated by a Scanning Tunneling Microscope. Angewandte Chemie - International Edition, 2013, 52, 4814-4817.	7.2	22
344	Rainfall facilitates the transmission and proliferation of antibiotic resistance genes from ambient air to soil. Science of the Total Environment, 2021, 799, 149260.	3.9	22
345	Effects of field-induced geometry relaxation on the electron transport properties of 4,4′-biphenyldithiol molecular junction. Chemical Physics Letters, 2007, 447, 69-73.	1.2	21
346	Mechanism for tautomerization induced conductance switching of naphthalocyanin molecule. Applied Physics Letters, 2009, 95, 182103.	1.5	21
347	Maximizing Integrated Optical and Electrical Properties of a Single ZnO Nanowire through Native Interfacial Doping. Advanced Materials, 2014, 26, 3035-3041.	11.1	21
348	Direct Determination of Resonance Energy Transfer in Photolyase: Structural Alignment for the Functional State. Journal of Physical Chemistry A, 2014, 118, 10522-10530.	1.1	21
349	Wafer scale fabrication of highly dense and uniform array of sub-5 nm nanogaps for surface enhanced Raman scatting substrates. Optics Express, 2016, 24, 20808.	1.7	21
350	Theoretical Isomer Identification of Three C <sub>56</sub> Fullerenes and Their Chlorinated Derivatives by XPS and NEXAFS Spectra. Journal of Physical Chemistry C, 2016, 120, 13779-13786.	1.5	21
351	DFT Studies on the Polymerization of Functionalized Styrenes Catalyzed by Rare-Earth-Metal Complexes: Factors Affecting C–H Activation Relevant to Step-Growth Polymerization. Organometallics, 2018, 37, 3210-3218.	1.1	21
352	Chemical Versatility of [FeFe]-Hydrogenase Models: Distinctive Activity of [μ-C6H4-1,2-(κ2-S)2][Fe2(CO)6] for Electrocatalytic CO2Reduction. ACS Catalysis, 2019, 9, 768-774.	5.5	21
353	lonic Liquid Enriches the Antibiotic Resistome, Especially Efflux Pump Genes, Before Significantly Affecting Microbial Community Structure. Environmental Science & Technology, 2020, 54, 4305-4315.	4.6	21
354	Role of non-Condon vibronic coupling and conformation change on two-photon absorption spectra of green fluorescent protein. Molecular Physics, 2013, 111, 1316-1321.	0.8	20
355	Identification of Free OH and its Implication on Structural Changes of Liquid Water. Chinese Journal of Chemical Physics, 2013, 26, 121-127.	0.6	20
356	Impact of Element Doping on Photoexcited Electron Dynamics in CdS Nanocrystals. Journal of Physical Chemistry Letters, 2017, 8, 5680-5686.	2.1	20
357	Cobalt-catalysed unactivated C(sp <sup>3</sup> )–H amination: two-state reactivity and multi-reference electronic character. Catalysis Science and Technology, 2019, 9, 1879-1890.	2.1	20
358	Antibiotic Resistance and Virulence of Extraintestinal Pathogenic Escherichia coli (ExPEC) Vary According to Molecular Types. Frontiers in Microbiology, 2020, 11, 598305.	1.5	20
359	Three-Branched Dendritic Dipolar Nonlinear Optical Chromophores, More than Three Times a Single-Strand Chromophore?. Journal of Physical Chemistry B, 2008, 112, 14751-14761.	1.2	19
360	Effects of Structural Fluctuations on Two-Photon Absorption Activity of Interacting Dipolar Chromophores. Journal of Physical Chemistry B, 2010, 114, 10814-10820.	1.2	19

#	Article	IF	CITATIONS
361	Electronic structure of bismuth telluride quasi-two-dimensional crystal: A first principles study. Applied Physics Letters, 2011, 98, .	1.5	19
362	Multidecker Bis(benzene)chromium: Opportunities for Design of Rigid and Highly Flexible Molecular Wires. Journal of Physical Chemistry C, 2011, 115, 785-790.	1.5	19
363	Tetranuclear Zirconium and Hafnium Polyhydride Complexes Composed of the "CpMH <sub>2</sub> ― Units. Organometallics, 2013, 32, 2145-2151.	1.1	19
364	Molecular molds for regularizing Kondo states at atom/metal interfaces. Nature Communications, 2020, 11, 2566.	5.8	19
365	Dinitrogen Cleavage and Functionalization with Carbon Dioxide in a Dititanium Dihydride Framework. Journal of the American Chemical Society, 2022, 144, 6972-6980.	6.6	19
366	Wavelike electronic energy transfer in donor–acceptor molecular systems through quantum coherence. Nature Nanotechnology, 2022, 17, 729-736.	15.6	19
367	DNA Repair by Spore Photoproduct Lyase:Â A Density Functional Theory Study. Journal of Physical Chemistry B, 2003, 107, 11188-11192.	1.2	18
368	Stabilizing single-molecular Raman spectrum of a nonbonding molecule on Ag nanoparticles. Chemical Communications, 2009, , 1342.	2.2	18
369	Hybrid molecular dynamics and first-principles study on the work function of a Pt(111) electrode immersed in aqueous solution at room temperature. Physical Review B, 2012, 86, .	1.1	18
370	Time-Dependent Wave Packet Quantum and Quasi-Classical Trajectory Study of He + H <sub>2</sub> <sup>+</sup> , D <sub>2</sub> <sup>+</sup> â†' HeH <sup>+</sup> + H, HeD <sup>+</sup> + D Reaction on an Accurate FCI Potential Energy Surface. Journal of Physical Chemistry A, 2012, 116, 2388-2393.	1.1	18
371	Electronic transport through zigzag/armchair graphene nanoribbon heterojunctions. Journal of Physics Condensed Matter, 2012, 24, 095801.	0.7	18
372	Gas-phase IR spectroscopy of deprotonated amino acids: Global or Local minima?. Chemical Physics Letters, 2014, 598, 86-90.	1.2	18
373	Study of double core hole excitations in molecules by X-ray double-quantum-coherence signals: a multi-configuration simulation. Chemical Science, 2016, 7, 5922-5933.	3.7	18
374	Determining the Chargeâ€Transfer Direction in a p–n Heterojunction BiOCl/g <sub>3</sub> N <sub>4</sub> Photocatalyst by Ultrafast Spectroscopy. ChemPhotoChem, 2017, 1, 350-354.	1.5	18
375	Suppressing Electron–Phonon Coupling through Laser-Induced Phase Transition. ACS Applied Materials & Interfaces, 2017, 9, 23309-23313.	4.0	18
376	A molecular-scale study on the hydration of sulfuric acid-amide complexes and the atmospheric implication. Chemosphere, 2018, 213, 453-462.	4.2	18
377	Atmospheric implications of hydration on the formation of methanesulfonic acid and methylamine clusters: A theoretical study. Chemosphere, 2020, 244, 125538.	4.2	18
378	Using Machine Learning to Predict the Dissociation Energy of Organic Carbonyls. Journal of Physical Chemistry A, 2020, 124, 3844-3850.	1.1	18

#	Article	IF	CITATIONS
379	Raman Detection of Bond Breaking and Making of a Chemisorbed Up-Standing Single Molecule at Single-Bond Level. Journal of Physical Chemistry Letters, 2021, 12, 1961-1968.	2.1	18
380	Colonization of gut microbiota by plasmid-carrying bacteria is facilitated by evolutionary adaptation to antibiotic treatment. ISME Journal, 2022, 16, 1284-1293.	4.4	18
381	Characteristics of Wild Bird Resistomes and Dissemination of Antibiotic Resistance Genes in Interconnected Bird-Habitat Systems Revealed by Similarity of <i>bla</i> <sub>TEM</sub> Polymorphic Sequences. Environmental Science & Technology, 2022, 56, 15084-15095.	4.6	18
382	Molecular Dynamics Simulations Applied to Electric Field Induced Second Harmonic Generation in Dipolar Chromophore Solutions. Journal of Physical Chemistry B, 2006, 110, 8971-8977.	1.2	17
383	Theoretical studies on the isomerization mechanism of the ortho-green fluorescent protein chromophore. Physical Chemistry Chemical Physics, 2012, 14, 13409.	1.3	17
384	Identification of the Scaling Relations for Binary Noble-Metal Nanoparticles. Journal of Physical Chemistry C, 2013, 117, 2849-2854.	1.5	17
385	Theoretical Identification of Three C <sub>66</sub> Fullerene Isomers and Related Chlorinated Derivatives by X-ray Photoelectron Spectroscopy and Near-edge X-ray Absorption Fine Structure Spectroscopy. Journal of Physical Chemistry A, 2016, 120, 9932-9940.	1.1	17
386	Structure-dependent photocatalytic decomposition of formic acid on the anatase TiO2(101) surface and strategies to increase its reaction rate. Journal of Power Sources, 2016, 306, 208-212.	4.0	17
387	Role of Hydrogen Bonding in Green Fluorescent Protein-like Chromophore Emission. Scientific Reports, 2019, 9, 11640.	1.6	17
388	Capping experiments reveal multiple surface active sites in CeO <sub>2</sub> and their cooperative catalysis. RSC Advances, 2019, 9, 15229-15237.	1.7	17
389	Imaging Tumorous Methylglyoxal by an Activatable Near-Infrared Fluorescent Probe for Monitoring Glyoxalase 1 Activity. Analytical Chemistry, 2019, 91, 15577-15584.	3.2	17
390	Emerging linear activity trend in the oxygen evolution reaction with dual-active-sites mechanism. Journal of Materials Chemistry A, 2020, 8, 20946-20952.	5.2	17
391	Significant higher airborne antibiotic resistance genes and the associated inhalation risk in the indoor than the outdoor. Environmental Pollution, 2021, 268, 115620.	3.7	17
392	Synergistic Effect of Boron Nitride and Carbon Domains in Boron Carbide Nitride Nanotube Supported Singleâ€Atom Catalysts for Efficient Nitrogen Fixation. Chemistry - A European Journal, 2021, 27, 6945-6953.	1.7	17
393	Emission rates for electron tunneling from InAs quantum dots to GaAs substrate. Journal of Applied Physics, 2004, 96, 6477-6481.	1.1	16
394	A Five-Center Rather than a Four-Center Transition State for Alkene Insertion into the Metalâ~'Alkyl Bond of a Cationic Binuclear Yttrium Complex. Organometallics, 2006, 25, 6162-6165.	1.1	16
395	An efficient firstâ€principle approach for electronic structures calculations of nanomaterials. Journal of Computational Chemistry, 2008, 29, 434-444.	1.5	16
396	Identification of Switching Mechanism in Molecular Junctions by Inelastic Electron Tunneling Spectroscopy. Journal of Physical Chemistry C, 2008, 112, 11018-11022.	1.5	16

#	Article	IF	CITATIONS
397	Effects of intermolecular interaction on inelastic electron tunneling spectra. Journal of Chemical Physics, 2008, 128, 064705.	1.2	16
398	Ultrafast deactivation processes in the 2-aminopyridine dimer and the adenine-thymine base pair: Similarities and differences. Journal of Chemical Physics, 2010, 133, 064302.	1.2	16
399	Importance of the Intramolecular Hydrogen Bond on the Photochemistry of Anionic Hydroquinone (FADH <sup>â^'</sup> ) in DNA Photolyase. Journal of Physical Chemistry Letters, 2010, 1, 743-747.	2.1	16
400	Photoassisted Magnetization of Fullerene C60 with Magnetic-Field Trapped Raman Scattering. Journal of the American Chemical Society, 2012, 134, 1130-1135.	6.6	16
401	Ferrate( <scp>vi</scp> ) initiated oxidative degradation mechanisms clarified by DFT calculations: a case for sulfamethoxazole. Environmental Sciences: Processes and Impacts, 2017, 19, 370-378.	1.7	16
402	Optomagnetic Effect Induced by Magnetized Nanocavity Plasmon. Journal of the American Chemical Society, 2019, 141, 13795-13798.	6.6	16
403	Azo-Dimerization Mechanisms of <i>p</i> -Aminothiophenol and <i>p</i> -Nitrothiophenol Molecules on Plasmonic Metal Surfaces Revealed by Tip-/Surface-Enhanced Raman Spectroscopy. Journal of Physical Chemistry C, 2020, 124, 11586-11594.	1.5	16
404	Theoretical Studies of Rare-Earth-Catalyzed [3 + 2] Annulation of Aromatic Aldimine with Styrene: Mechanism and Origin of Diastereoselectivity. Journal of Organic Chemistry, 2021, 86, 4236-4244.	1.7	16
405	Hydrogenated Oxide Material for Selfâ€Targeting and Automaticâ€Degrading Photothermal Tumor Therapy in the NIRâ€II Bioâ€Window. Advanced Functional Materials, 2022, 32, .	7.8	16
406	Solvent Effects on the Three-Photon Absorption of a Symmetric Charge-Transfer Molecule. Journal of Physical Chemistry B, 2008, 112, 4703-4710.	1.2	15
407	Structures of Water Molecules Adsorbed on a Gold Electrode under Negative Potentials. Journal of Physical Chemistry C, 2010, 114, 4051-4056.	1.5	15
408	Strong current polarization and negative differential resistance in chiral graphene nanoribbons with reconstructed (2,1)-edges. Applied Physics Letters, 2012, 101, 073101.	1.5	15
409	DFT Studies on the Methane Elimination Reaction of a Trinuclear Rare-Earth Polymethyl Complex: σ-Bond Metathesis Assisted by Cooperation of Multimetal Sites. Organometallics, 2014, 33, 1126-1134.	1.1	15
410	Isomer-Dependent Franck–Condon Blockade in Weakly Coupled Bipyridine Molecular Junctions. Journal of Physical Chemistry C, 2014, 118, 14853-14859.	1.5	15
411	Highly selective trifluoroacetic ester/ketone metathesis: an efficient approach to trifluoromethyl ketones and esters. Tetrahedron, 2014, 70, 4668-4674.	1.0	15
412	Significant Contributions of the Albrecht's <i>A</i> Term to Nonresonant Raman Scattering Processes. Journal of Chemical Theory and Computation, 2015, 11, 5385-5390.	2.3	15
413	Theoretical Investigations of Isoprene Polymerization Catalyzed by Cationic Half-Sandwich Scandium Complexes Bearing a Coordinative Side Arm. Organometallics, 2018, 37, 551-558.	1.1	15
414	"C–Hâ<¯ï€ Interaction―regulates the stereoselectivity in olefin polymerization. Chemical Communications, 2019, 55, 6689-6692.	2.2	15

#	Article	IF	CITATIONS
415	Theoretical study of the hydration effects on alkylamine and alkanolamine clusters and the atmospheric implication. Chemosphere, 2020, 243, 125323.	4.2	15
416	Spin Polarization-Induced Facile Dioxygen Activation in Boron-Doped Graphitic Carbon Nitride. ACS Applied Materials & Interfaces, 2020, 12, 52741-52748.	4.0	15
417	Monitoring antibiotic resistomes and bacterial microbiomes in the aerosols from fine, hazy, and dusty weather in Tianjin, China using a developed high-volume tandem liquid impinging sampler. Science of the Total Environment, 2020, 731, 139242.	3.9	15
418	Seasonal disparities and source tracking of airborne antibiotic resistance genes in Handan, China. Journal of Hazardous Materials, 2022, 422, 126844.	6.5	15
419	The impact of COVID-19 on urban PM2.5 —taking Hubei Province as an example. Environmental Pollution, 2022, 294, 118633.	3.7	15
420	Nanomechanically induced molecular conductance switch. Applied Physics Letters, 2009, 95, 232118.	1.5	14
421	Effects of Coexisting Isomers on Two-Photon Absorption of Organic Molecules in Solutions. Journal of Physical Chemistry B, 2010, 114, 13167-13172.	1.2	14
422	Coherent interference in the resonant dissociative electron attachment to carbon monoxide. Physical Review A, 2013, 88, .	1.0	14
423	Cluster approximations of chemically enhanced molecule-surface Raman spectra: The case of trans-1,2-bis (4-pyridyl) ethylene (BPE) on gold. Chemical Physics Letters, 2013, 581, 70-73.	1.2	14
424	Regio- and stereospecific living polymerization and copolymerization of (E)-1,3-pentadiene with 1,3-butadiene by half-sandwich scandium catalysts. Dalton Transactions, 2013, 42, 9030.	1.6	14
425	Fe L-Edge X-ray Absorption Spectra of Fe(II) Polypyridyl Spin Crossover Complexes from Time-Dependent Density Functional Theory. Journal of Physical Chemistry A, 2013, 117, 14075-14085.	1.1	14
426	Molecular Design to Enhance the Thermal Stability of a Photo Switchable Molecular Junction Based on Dimethyldihydropyrene and Cyclophanediene Isomerization. Journal of Physical Chemistry C, 2015, 119, 11468-11474.	1.5	14
427	Strong Fermi level pinning induces a high rectification ratio and negative differential resistance in hydrogen bonding bridged single cytidine pair junctions. Physical Chemistry Chemical Physics, 2016, 18, 26586-26594.	1.3	14
428	Theoretical identification of C34 isomers by XPS and NEXAFS spectra. Chemical Physics Letters, 2016, 644, 111-116.	1.2	14
429	Lighting up long-range charge-transfer states by a localized plasmonic field. Nanoscale, 2017, 9, 18189-18193.	2.8	14
430	First-principles study on the mechanism of photocatalytic reduction of nitrobenzene on the rutile TiO <sub>2</sub> (110) surface. Physical Chemistry Chemical Physics, 2020, 22, 1187-1193.	1.3	14
431	Mechanistic Studies for Palladium Catalyzed Copolymerization of Ethylene with Vinyl Ethers. Polymers, 2020, 12, 2401.	2.0	14
432	A Kinetic View on Proximity-Dependent Selectivity of Carbon Dioxide Reduction on Bifunctional Catalysts. ACS Catalysis, 2020, 10, 13518-13523.	5.5	14

#	Article	IF	CITATIONS
433	Colonization of Mice With Amoxicillin-Associated Klebsiella variicola Drives Inflammation via Th1 Induction and Treg Inhibition. Frontiers in Microbiology, 2020, 11, 1256.	1.5	14
434	Colistin and amoxicillin combinatorial exposure alters the human intestinal microbiota and antibiotic resistome in the simulated human intestinal microbiota. Science of the Total Environment, 2021, 750, 141415.	3.9	14
435	On-Surface Debromination of C <sub>6</sub> Br <sub>6</sub> : C <sub>6</sub> Ring versus C <sub>6</sub> Chain. ACS Nano, 2022, 16, 6578-6584.	7.3	14
436	Multidimensional transition-state theory calculations for nuclear dynamics of core-excited molecules. Physical Review A, 2004, 70, .	1.0	13
437	Understanding the scattering mechanism of single-walled carbon nanotube based gas sensors. Carbon, 2010, 48, 1970-1976.	5.4	13
438	Repair of DNA Dewar Photoproduct to (6-4) Photoproduct in (6-4) Photolyase. Journal of Physical Chemistry B, 2011, 115, 10976-10982.	1.2	13
439	A fragment based step-by-step strategy for determining the most stable conformers of biomolecules. Chemical Physics Letters, 2014, 610-611, 303-309.	1.2	13
440	Complete Nucleotide Sequence of pGA45, a 140,698-bp IncFIIY Plasmid Encoding blaIMI-3-Mediated Carbapenem Resistance, from River Sediment. Frontiers in Microbiology, 2016, 7, 188.	1.5	13
441	Theoretical modeling of surface and tipâ€enhanced Raman spectroscopies. Wiley Interdisciplinary Reviews: Computational Molecular Science, 2017, 7, e1293.	6.2	13
442	Uniform and perfectly linear current–voltage characteristics of nitrogen-doped armchair graphene nanoribbons for nanowires. Physical Chemistry Chemical Physics, 2017, 19, 44-48.	1.3	13
443	Identification of the protonation site of gaseous triglycine: the cis-peptide bond conformation as the global minimum. Physical Chemistry Chemical Physics, 2017, 19, 15030-15038.	1.3	13
444	DFT Studies on cis-1,4-Polymerization of Dienes Catalyzed by a Cationic Rare-Earth Metal Complex Bearing an Ancillary PNP Ligand. Polymers, 2017, 9, 53.	2.0	13
445	The widening urbanization gap between the Three Northeast Provinces and the Yangtze River Delta under China's economic reform from 1984 to 2014. International Journal of Sustainable Development and World Ecology, 2018, 25, 262-275.	3.2	13
446	Theoretical Mechanistic Studies on Redox-Switchable Polymerization of Trimethylene Carbonate Catalyzed by an Indium Complex Bearing a Ferrocene-Based Ligand. Organometallics, 2018, 37, 4599-4607.	1.1	13
447	Utilization of Resist Stencil Lithography for Multidimensional Fabrication on a Curved Surface. ACS Nano, 2018, 12, 9626-9632.	7.3	13
448	Thermally Activated Delayed Fluorescence in an Organic Cocrystal: Narrowing the Singlet–Triplet Energy Gap via Charge Transfer. Angewandte Chemie, 2019, 131, 11433.	1.6	13
449	Amoxicillin Increased Functional Pathway Genes and Beta-Lactam Resistance Genes by Pathogens Bloomed in Intestinal Microbiota Using a Simulator of the Human Intestinal Microbial Ecosystem. Frontiers in Microbiology, 2020, 11, 1213.	1.5	13
450	Primary and Secondary Succession Mediate the Accumulation of Biogenic Amines during Industrial Semidry Chinese Rice Wine Fermentation. Applied and Environmental Microbiology, 2020, 86, .	1.4	13

#	Article	IF	CITATIONS
451	Fragmentation Mechanism of White Phosphorus: A Theoretical Insight into Multiple Cleavage/Formation of Pâ^'P and Pâ^'C Bonds. Chemistry - A European Journal, 2020, 26, 13282-13287.	1.7	13
452	Computational study of the copolymerization mechanism of ethylene with methyl 2-acetamidoacrylate catalyzed by phosphine-sulfonate palladium complexes. New Journal of Chemistry, 2021, 45, 16670-16678.	1.4	13
453	Quasi-Analytical Approach for Modeling of Surface-Enhanced Raman Scattering. Journal of Physical Chemistry C, 2015, 119, 28992-28998.	1.5	13
454	Study of Double-Side Ultrasonic Embossing for Fabrication of Microstructures on Thermoplastic Polymer Substrates. PLoS ONE, 2013, 8, e61647.	1.1	13
455	Aggregation effects on two-photon absorption spectra of octupolar molecules. Journal of Chemical Physics, 2007, 127, 026101.	1.2	12
456	DFT Study on Isomerization and Decomposition of Cuprous Dialkyldithiophosphate and Its Reaction with Alkylperoxy Radical. Journal of Physical Chemistry A, 2008, 112, 5720-5726.	1.1	12
457	Nonradiative decay of the lowest excited singlet state of 2-aminopyridine is considerably faster than the radiative decay. Journal of Chemical Physics, 2009, 130, 144315.	1.2	12
458	Electronic structure of [121]tetramantane-6-thiol on gold and silver surfaces. Journal of Chemical Physics, 2009, 130, 054705.	1.2	12
459	Simulation of inelastic electronic tunneling spectra of adsorbates from first principles. Journal of Chemical Physics, 2009, 130, 134707.	1.2	12
460	Molecular Dynamics and Quantum Chemistry Study on Conformations and Optical Properties of Hydrogen Bonded Dipolar Merocyanine Dyes. Journal of Physical Chemistry B, 2009, 113, 10271-10276.	1.2	12
461	Elastic and inelastic electron transport in metal–molecule(s)–metal junctions. Physica E: Low-Dimensional Systems and Nanostructures, 2013, 47, 167-187.	1.3	12
462	Enhanced Horizontal Transfer of Antibiotic Resistance Genes in Freshwater Microcosms Induced by an Ionic Liquid. PLoS ONE, 2015, 10, e0126784.	1.1	12
463	Vibrational identification for conformations of trans-1,2-bis (4-pyridyl) ethylene in gold molecular junctions. Chemical Physics, 2015, 453-454, 20-25.	0.9	12
464	Mechanism of two-photon excited hemoglobin fluorescence emission. Journal of Biomedical Optics, 2015, 20, 105014.	1.4	12
465	Non-selective Separation of Bacterial Cells with Magnetic Nanoparticles Facilitated by Varying Surface Charge. Frontiers in Microbiology, 2016, 7, 1891.	1.5	12
466	Gauge invariant theory for super high resolution Raman images. Journal of Chemical Physics, 2017, 146, 194106.	1.2	12
467	Identifying the structure of 4-chlorophenyl isocyanide adsorbed on Au(111) and Pt(111) surfaces by first-principles simulations of Raman spectra. Physical Chemistry Chemical Physics, 2017, 19, 32389-32397.	1.3	12
468	Theoretical modeling of tip-enhanced resonance Raman images of switchable azobenzene molecules on Au(111). Nanoscale, 2018, 10, 11850-11860.	2.8	12

#	Article	IF	CITATIONS
469	Origin of Product Selectivity in Yttrium-Catalyzed Benzylic C–H Alkylations of Alkylpyridines with Olefins: A DFT Study. Organometallics, 2018, 37, 2741-2748.	1.1	12
470	Neurological manifestations of autoinflammatory diseases in Chinese adult patients. Seminars in Arthritis and Rheumatism, 2020, 50, 1500-1506.	1.6	12
471	Photoinduced Formation of N2Molecules in Ammonium Compounds. Journal of Physical Chemistry A, 2007, 111, 9662-9669.	1.1	11
472	A density functional theory study of shake-up satellites in photoemission of carbon fullerenes and nanotubes. Journal of Chemical Physics, 2008, 128, 234704.	1.2	11
473	Important Structural Factors Controlling the Conductance of DNA Pairs in Molecular Junctions. Journal of Physical Chemistry C, 2010, 114, 14240-14242.	1.5	11
474	Effects of Interface Roughness on Electronic Transport Properties of Nanotubeâ^'Moleculeâ^'Nanotube Junctions. Journal of Physical Chemistry C, 2010, 114, 12335-12340.	1.5	11
475	Understanding the concept of randomness in inelastic electron tunneling excitations. Physical Chemistry Chemical Physics, 2010, 12, 12012.	1.3	11
476	Molecular polarization bridging physical and chemical enhancements in surface enhanced Raman scattering. Chemical Communications, 2011, 47, 11438.	2.2	11
477	Theoretical mechanistic studies on the degradation of alizarin yellow R initiated by hydroxyl radical. Journal of Physical Organic Chemistry, 2014, 27, 519-526.	0.9	11
478	Note: Coherent resonances observed in the dissociative electron attachment to carbon monoxide. Journal of Chemical Physics, 2015, 143, 066101.	1.2	11
479	Mechanistic Insights into the Methylenation of Ketone by a Trinuclear Rare-Earth-Metal Methylidene Complex. Organometallics, 2015, 34, 366-372.	1.1	11
480	Optical Excitation in Donor–Pt–Acceptor Complexes: Role of the Structure. Journal of Physical Chemistry A, 2016, 120, 3547-3553.	1.1	11
481	Mechanistic insights into regioselective polymerization of 1,3-Dienes catalyzed by a bipyridine-ligated iron complex: A DFT study. International Journal of Quantum Chemistry, 2016, 116, 1274-1280.	1.0	11
482	Spatiotemporal patterns of PM2.5 in the Beijing–Tianjin–Hebei region during 2013–2016. , 2017, 1, 95-10	3.	11
483	Self-Adaptive Switch Enabling Complete Charge Separation in Molecular-Based Optoelectronic Conversion. Journal of Physical Chemistry Letters, 2018, 9, 837-843.	2.1	11
484	Clinical and genetic features of Chinese adult patients with tumour necrosis factor receptor-associated periodic fever syndrome. Rheumatology, 2020, 59, 1969-1974.	0.9	11
485	Field effects on the statistical behavior of the molecular conductance in a single molecular junction in aqueous solution. Nano Research, 2010, 3, 350-355.	5.8	10
486	Tuning the Electronic Transport Properties of Zigzag Graphene Nanoribbons via Hydrogenation Separators. Journal of Physical Chemistry C, 2011, 115, 24366-24372.	1.5	10

#	Article	IF	CITATIONS
487	Local Structures and Chemical Properties of Deprotonated Arginine. Chinese Journal of Chemical Physics, 2012, 25, 681-686.	0.6	10
488	Advanced experimental methods toward understanding biophysicochemical interactions of interfacial biomolecules by using sum frequency generation vibrational spectroscopy. Science China Chemistry, 2014, 57, 1646-1661.	4.2	10
489	Tuning electronic and magnetic properties of armchair   zigzag hybrid graphene nanoribbons by the choice of supercell model of grain boundaries. Journal of Applied Physics, 2014, 115, 104303.	1.1	10
490	Shape-Dependent Electronic Excitations in Metallic Chains. Journal of Physical Chemistry C, 2014, 118, 13059-13069.	1.5	10
491	Remarkable enhancement of photovoltaic performance of ZnO/CdTe core–shell nanorod array solar cells through interface passivation with a TiO2 layer. RSC Advances, 2015, 5, 71883-71889.	1.7	10
492	Retrieving the Rate of Reverse Intersystem Crossing from Ultrafast Spectroscopy. Journal of Physical Chemistry Letters, 2016, 7, 3908-3912.	2.1	10
493	Surface Plasmon Assisted Directional Rayleigh Scattering. Chinese Journal of Chemical Physics, 2017, 30, 135-138.	0.6	10
494	Energy Materials Design for Steering Charge Kinetics. Advanced Materials, 2018, 30, e1801988.	11.1	10
495	Bifacial Raman Enhancement on Monolayer Two-Dimensional Materials. Nano Letters, 2019, 19, 1124-1130.	4.5	10
496	Theoretical Insights into Olefin Polymerization Catalyzed by Cationic Organo Rare-Earth Metal Complexes. , 2019, , 327-356.		10
497	Direct Donation of Protons from H <sub>2</sub> 0 to CO <sub>2</sub> in Artificial Photosynthesis on the Anatase TiO <sub>2</sub> (101) Surface. Journal of Physical Chemistry C, 2019, 123, 3019-3023.	1.5	10
498	Selectively Scissoring Hydrogen-Bonded Cytosine Dimer Structures Catalyzed by Water Molecules. ACS Nano, 2020, 14, 10680-10687.	7.3	10
499	Amorphous TiO2 as a multifunctional interlayer for boosting the efficiency and stability of the CdS/cobaloxime hybrid system for photocatalytic hydrogen production. Nanoscale, 2020, 12, 11267-11279.	2.8	10
500	Advancing conjugated polymers into nanometer-scale devices. Pure and Applied Chemistry, 2006, 78, 1803-1822.	0.9	9
501	Determination of the Configuration of a Single Molecule Junction by Inelastic Electron Tunneling Spectroscopy. Journal of Physical Chemistry C, 2010, 114, 5199-5202.	1.5	9
502	Super-long barnesite Na2V6O16·3H2O nanobelts for aligned film electrodes with enhanced anisotropic electrical transport. RSC Advances, 2012, 2, 7290.	1.7	9
503	Nonlinear inelastic electron scattering revealed byÂplasmon-enhanced electron energy-loss spectroscopy. Nature Physics, 2014, 10, 753-757.	6.5	9
504	Complete Nucleotide Sequence of IncP-1Î <sup>2</sup> Plasmid pDTC28 Reveals a Non-Functional Variant of the blaGES-Type Gene. PLoS ONE, 2016, 11, e0154975.	1.1	9

#	Article	IF	CITATIONS
505	Effects of domain size on x-ray absorption spectra of boron nitride doped graphenes. Applied Physics Letters, 2016, 109, .	1.5	9
506	Synthesis of Ferrocenyl-Based Unsymmetrical Azines via a Simple Reaction of Aldehydes with Ketone-Derived <i>N</i> -Tosyl Hydrazones and the Evaluation of the Extent of Conjugation in the Molecule. Organometallics, 2017, 36, 3215-3225.	1.1	9
507	E–H (E = N and P) Bond Activation of PhEH <sub>2</sub> by a Trinuclear Yttrium Methylidene Complex: Theoretical Insights into Mechanism and Multimetal Cooperation Behavior. Organometallics, 2017, 36, 4611-4619.	1.1	9
508	Computational Studies on the Selective Polymerization of Lactide Catalyzed by Bifunctional Yttrium NHC Catalyst. Inorganics, 2017, 5, 46.	1.2	9
509	Effects of Ligand, Metal, and Solvation on the Structure and Stability of Contact Ion Pairs Relevant to Olefin Polymerization Catalyzed by Rare-Earth-Metal Complexes: A DFT Study. Organometallics, 2018, 37, 882-890.	1.1	9
510	B(C 6 F 5 ) 3 /Amine atalyzed C(sp)â^'H Silylation of Terminal Alkynes with Hydrosilanes: Experimental and Theoretical Studies. Angewandte Chemie, 2018, 130, 15442-15446.	1.6	9
511	Physically Close yet Chemically Separate Reduction and Oxidation Sites in Double-Walled Nanotubes for Photocatalytic Hydrogen Generation. Journal of Physical Chemistry Letters, 2019, 10, 3739-3743.	2.1	9
512	Formation of polyynes and ring-polyyne molecules following fragmentation of polycyclic aromatic hydrocarbons. Monthly Notices of the Royal Astronomical Society, 2019, 486, 1875-1881.	1.6	9
513	Monitoring Hydrogen/Deuterium Tautomerization in Transient Isomers of Single Porphine by Highly Localized Plasmonic Field. Journal of Physical Chemistry C, 2019, 123, 11081-11093.	1.5	9
514	Origin of stereoselectivity and multidimensional quantitative analysis of ligand effects on yttrium-catalysed polymerization of 2-vinylpyridine. Catalysis Science and Technology, 2019, 9, 6227-6233.	2.1	9
515	Sharp-tip enhanced catalytic CO oxidation by atomically dispersed Pt <sub>1</sub> /Pt <sub>2</sub> on a raised graphene oxide platform. Journal of Materials Chemistry A, 2020, 8, 12485-12494.	5.2	9
516	Ketones as Molecular Coâ€catalysts for Boosting Excitonâ€Based Photocatalytic Molecular Oxygen Activation. Angewandte Chemie, 2020, 132, 11186-11193.	1.6	9
517	Highly Sensitive, Selective, Flexible and Scalable Room-Temperature NO2 Gas Sensor Based on Hollow SnO2/ZnO Nanofibers. Molecules, 2021, 26, 6475.	1.7	9
518	Graphene-controlled FeSe nanoparticles embedded in carbon nanofibers for high-performance potassium-ion batteries. Science China Materials, 2022, 65, 1751-1760.	3.5	9
519	Decomposition of alkyl hydroperoxide by a copper(I) complex: insights from density functional theory. Tetrahedron Letters, 2008, 49, 6841-6845.	0.7	8
520	Basis set dependence of solute–solvent interaction energy of benzene in water: A HF/DFT study. Journal of Computational Chemistry, 2008, 29, 1725-1732.	1.5	8
521	Molecular modeling of inelastic electron transport in molecular junctions. Journal of Physics Condensed Matter, 2008, 20, 374110.	0.7	8
522	Intrinsic Property of Flavin Mononucleotide Controls its Optical Spectra in Three Redox States. ChemPhysChem, 2011, 12, 2899-2902.	1.0	8

#	Article	IF	CITATIONS
523	Effect of reagent vibrational excitation and isotope substitution on the stereo-dynamics of the Ba + HF → BaF + H reaction. Chinese Physics B, 2011, 20, 043402.	0.7	8
524	Spectral character of intermediate state in solid-state photoarrangement of α-santonin. Chemical Physics, 2012, 405, 40-45.	0.9	8
525	Quantum Effects on Global Structure of Liquid Water. Chinese Journal of Chemical Physics, 2013, 26, 127-132.	0.6	8
526	RRS-PBC: a molecular approach for periodic systems. Science China Chemistry, 2014, 57, 1399-1404.	4.2	8
527	The effect of Duschinsky rotation on charge transport properties of molecular junctions in the sequential tunneling regime. Physical Chemistry Chemical Physics, 2015, 17, 23007-23016.	1.3	8
528	Bringing light into the dark triplet space of molecular systems. Physical Chemistry Chemical Physics, 2015, 17, 13129-13136.	1.3	8
529	Identification of the smallest peptide with a zwitterion as the global minimum: a first-principles study on arginine-containing peptides. Physical Chemistry Chemical Physics, 2017, 19, 12117-12126.	1.3	8
530	Unraveling the Mechanism for the Sharpâ€īp Enhanced Electrocatalytic Carbon Dioxide Reduction: The Kinetics Decide. Angewandte Chemie, 2017, 129, 15823-15827.	1.6	8
531	Metal impacts on the persistence and proliferation of β-lactam resistance genes in Xiangjiang River, China. Environmental Science and Pollution Research, 2019, 26, 25208-25217.	2.7	8
532	Theoretical Mechanistic Insights into Dinitrogen Activation by a Diniobium Tetrahydride: Two-State Reactivity and the Role of Potassium Cation Promoter. Inorganic Chemistry, 2020, 59, 4626-4633.	1.9	8
533	Degradation of Polydienes Induced by Alkyllithium: Characterization and Reaction Mechanism. Macromolecules, 2021, 54, 1147-1158.	2.2	8
534	Are pyridinium ylides radicals?. Chemical Communications, 2020, 56, 11287-11290.	2.2	8
535	Conformational Order of Alkyl Side Chain of Poly(3-alkylthiophene) Promotes Hole-Extraction Ability in Perovskite/Poly(3-alkylthiophene) Heterojunction. Journal of Physical Chemistry Letters, 2021, 12, 11817-11823.	2.1	8
536	Optical Images of Molecular Vibronic Couplings from Tip-Enhanced Fluorescence Excitation Spectroscopy. Jacs Au, 2022, 2, 150-158.	3.6	8
537	Modeling η5 -C5 Me4 SiMe3 with η3 -C3 H5 for DFT study of a tetranuclear yttrium polyhydrido complex [(η5 -C5 Me4 SiMe3 )YH2 ]4. International Journal of Quantum Chemistry, 2007, 107, 374-381.	1.0	7
538	Two- and three-photon absorption of organic ionic pyrylium based materials. Journal of Chemical Physics, 2009, 130, 174312.	1.2	7
539	Density functional study on mechanism of CO oxidation with activated water on O/Au (111) surface. Science Bulletin, 2009, 54, 1973-1977.	4.3	7
540	Single Molecule's Conductance Depending On Its Orientation. Journal of Physical Chemistry C, 2009, 113, 26-30.	1.5	7

#	Article	IF	CITATIONS
541	Electronic structure of room-temperature ferromagnetic Mg <sub>1â^'x</sub> Fe <sub>x</sub> O <sub>y</sub> thin films. Applied Physics Letters, 2012, 101, 082411.	1.5	7
542	Theoretical Studies on the Photoinduced Rearrangement Mechanism of αâ€Santonin. ChemPhysChem, 2012, 13, 353-362.	1.0	7
543	The role of dimerization on the structure transformation of arginine in gas phase. Chemical Physics Letters, 2014, 608, 398-403.	1.2	7
544	A comparative theoretical study on core-hole excitation spectra of azafullerene and its derivatives. Journal of Chemical Physics, 2014, 140, 124304.	1.2	7
545	Theoretical Mechanistic Studies on Methyltrioxorhenium-Catalyzed Olefin Cyclopropanation: Stepwise Transfer of a Terminal Methylene Group. Organometallics, 2014, 33, 3840-3846.	1.1	7
546	Reply to ``Comment on `Coherent interference in the resonant dissociative electron attachment to carbon monoxide' ''. Physical Review A, 2015, 91, .	1.0	7
547	Theoretical spectroscopic studies on chemical and electronic structures of arginylglycine. Physical Chemistry Chemical Physics, 2015, 17, 24754-24760.	1.3	7
548	Synthesis and structure of the first discrete dinuclear cationic aluminum complexes. Dalton Transactions, 2016, 45, 12346-12351.	1.6	7
549	<scp>DFT</scp> Studies on Isoprene/Ethylene Copolymerization Catalyzed by Cationic Scandium Complexes Bearing Different Ancillary Ligands. Chinese Journal of Chemistry, 2017, 35, 723-732.	2.6	7
550	Theoretical simulations for vibrationally-resolved absorption spectra of naphthalenediimide cyclophane derivatives. Spectrochimica Acta - Part A: Molecular and Biomolecular Spectroscopy, 2017, 183, 339-347.	2.0	7
551	Effects of Plasmon Modes on Resonant Raman Images of a Single Molecule. Journal of Physical Chemistry Letters, 2020, 11, 407-411.	2.1	7
552	Creation of the Dirac Nodal Line by Extrinsic Symmetry Engineering. Nano Letters, 2020, 20, 2157-2162.	4.5	7
553	Rare-Earth Aryloxide/Ylide-Functionalized Phosphine Frustrated Lewis Pairs for the Polymerization of 4-Vinylpyridine and Its Derivatives. Macromolecules, 2021, 54, 7724-7731.	2.2	7
554	Long-term spatiotemporal variation of antimicrobial resistance genes within the Serratia marcescens population and transmission of S. marcescens revealed by public whole-genome datasets. Journal of Hazardous Materials, 2022, 423, 127220.	6.5	7
555	Origin of different chain-end microstructures in ethylene/vinyl halide copolymerization catalysed by phosphine–sulfonate palladium complexes. New Journal of Chemistry, 2020, 44, 16941-16947.	1.4	7
556	Identifying configuration and orientation of adsorbed molecules by inelastic electron tunneling spectra. Journal of Chemical Physics, 2010, 133, 064702.	1.2	6
557	Identification of 13- and 14-Coordinated Structures of First Hydrated Shell of [AuCl <sub>4</sub> ] <sup>â^'</sup> Acid Aqueous Solution by Combination of MD and XANES. Journal of Physical Chemistry B, 2012, 116, 7866-7873.	1.2	6
558	The complete mitochondrial genome ofTanakia limbata(Cypriniformes: Cyprinidae). Mitochondrial DNA, 2014, 27, 1-2.	0.6	6

#	Article	IF	CITATIONS
559	Complete nucleotide sequence of plasmid pNA6 reveals the high plasticity of IncU family plasmids. Gene, 2016, 591, 74-79.	1.0	6
560	Visualization of Vibrational Modes in Real Space by Tipâ€Enhanced Nonâ€Resonant Raman Spectroscopy. Angewandte Chemie, 2016, 128, 1053-1057.	1.6	6
561	Ultrafast Vibrational Dynamics of Membraneâ€Bound Peptides at the Lipid Bilayer/Water Interface. Angewandte Chemie, 2017, 129, 13157-13161.	1.6	6
562	A theoretical study on vibronic spectra and photo conversation process of protonated naphthalenes. Spectrochimica Acta - Part A: Molecular and Biomolecular Spectroscopy, 2018, 205, 520-527.	2.0	6
563	A novel energy-dependent p-semiconductor–metal–n-semiconductor heterojunction for selectively steering charge flow in a <i>Z</i> -scheme photocatalyst. Journal of Materials Chemistry A, 2019, 7, 15036-15041.	5.2	6
564	Mechanistic Insights into La-Catalyzed Amidation of Aldehyde with Amine. Organic Letters, 2020, 22, 705-708.	2.4	6
565	Synthesis of Thermoplastic Elastomers by Yttrium-Catalyzed Isospecific <i>Trans</i> -1,4-Polymerization of ( <i>E</i> )-1,3-Pentadiene. Bulletin of the Chemical Society of Japan, 2021, 94, 1285-1291.	2.0	6
566	Diboron-mediated palladium-catalyzed asymmetric transfer hydrogenation using the proton of alcohols as hydrogen source. Science China Chemistry, 2021, 64, 1743-1749.	4.2	6
567	Photodissociation of phosgene: Theoretical evidence for the ultrafast and synchronous concerted three-body process. Journal of Chemical Physics, 2009, 131, 164306.	1.2	5
568	Formation and electronic transport properties of bimolecular junctions based on aromatic coupling. Journal of Physics Condensed Matter, 2010, 22, 325102.	0.7	5
569	Assignments of Inelastic Electron Tunneling Spectra of Semifluorinated Alkanethiol Molecular Junctions. Journal of Physical Chemistry C, 2011, 115, 20301-20306.	1.5	5
570	Energy landscape inside the cage of neutral and charged N@C60. Chemical Physics Letters, 2011, 517, 199-203.	1.2	5
571	Conductivity of carbon-based molecular junctions from ab-initio methods. Frontiers of Physics, 2014, 9, 748-759.	2.4	5
572	Tuning electron transport through a single molecular junction by bridge modification. Journal of Applied Physics, 2014, 116, .	1.1	5
573	Polyphenylsilole multilayers – an insight from X-ray electron spectroscopy and density functional theory. Physical Chemistry Chemical Physics, 2015, 17, 31117-31124.	1.3	5
574	Systematic Study on Hydrated Arginine: Clear Theoretical Evidence for the Canonical-to-Zwitterionic Structure Transition. Journal of Physical Chemistry A, 2017, 121, 3598-3605.	1.1	5
575	Macroscopic Wires from Fluorophore-Quencher Dyads with Long-Lived Blue Emission. Journal of Physical Chemistry A, 2017, 121, 7183-7190.	1.1	5
576	Effects of nucleophilic ligands on the chain initiation efficiency of polar monomer polymerizations catalyzed by 2-methoxyethylaminobis(phenolate)yttrium complexes: a DFT study. Dalton Transactions, 2017, 46, 16993-16999.	1.6	5

#	Article	IF	CITATIONS
577	Tunable Single-Photon Emission by Defective Boron-Nitride Nanotubes for High-Precision Force Detection. Journal of Physical Chemistry C, 2019, 123, 9624-9628.	1.5	5
578	The Effect of the Polyaromatic Hydrocarbon in the Formation of Fullerenes. Angewandte Chemie - International Edition, 2020, 59, 3942-3947.	7.2	5
579	Regulation of Electronic Structure of Graphene Nanoribbon by Tuning Long-Range Dopant–Dopant Coupling at Distance of Tens of Nanometers. Journal of Physical Chemistry Letters, 2020, 11, 6907-6913.	2.1	5
580	Mechanism Study of Molecular Deformation of 2,2′,5′,2″-Tetramethylated <i>p</i> -Terphenyl-4,4″-dithi Trapped in Gold Junctions. Journal of Physical Chemistry Letters, 2020, 11, 4456-4461.	iol 2.1	5
581	Theoretical studies on the N–X (X = Cl, O) bond activation mechanism in catalytic C–H amination. Catalysis Science and Technology, 2020, 10, 1914-1924.	2.1	5
582	Theoretical insight into the opposite redox activity of iron complexes toward the ring opening polymerization of lactide and epoxide. Inorganic Chemistry Frontiers, 2021, 8, 1005-1014.	3.0	5
583	Copper-catalyzed four-component reaction of alkenes, Togni's reagent, amines and CO <sub>2</sub> : stereoselective synthesis of ( <i>Z</i> )-enol carbamates. Organic Chemistry Frontiers, 2021, 8, 1851-1857.	2.3	5
584	Edge-effect enhanced catalytic CO oxidation by atomically dispersed Pt on nitride-graphene. Journal of Materials Chemistry A, 2021, 9, 2093-2098.	5.2	5
585	Ocular manifestations in Chinese adult patients with NLRP3-associated autoinflammatory disease. Scientific Reports, 2021, 11, 11904.	1.6	5
586	Theoretical Insight into the Inelastic Electron Tunneling Spectra of an Anil Derivative. Journal of Physical Chemistry A, 2013, 117, 12783-12795.	1.1	4
587	Semiconductors: A Unique Semiconductor-Metal-Graphene Stack Design to Harness Charge Flow for Photocatalysis (Adv. Mater. 32/2014). Advanced Materials, 2014, 26, 5578-5578.	11.1	4
588	Effects of the basis set and of the exchange–correlation functional on the Inelastic Electron Tunneling signatures of 1,4-benzenedithiol. Spectrochimica Acta - Part A: Molecular and Biomolecular Spectroscopy, 2014, 119, 34-41.	2.0	4
589	Infrared spectra of small anionic water clusters from density functional theory and wavefunction theory calculations. Physical Chemistry Chemical Physics, 2015, 17, 12698-12707.	1.3	4
590	Understanding the magnetic interaction between intrinsic defects and impurity ions in room-temperature ferromagnetic Mg1â^'xFexO thin films. Journal of Physics Condensed Matter, 2016, 28, 156002.	0.7	4
591	Electronic Structure of Thiolateâ€bridged Diiron Complexes and a Singleâ€electron Oxidation Reaction: A Combination of Experimental and Computational Studies. Chinese Journal of Chemistry, 2016, 34, 919-924.	2.6	4
592	DFT studies on the origin of regioselective ring-opening of terminal epoxides during copolymerization with CO2. Chinese Journal of Polymer Science (English Edition), 2016, 34, 439-445.	2.0	4
593	A neural network protocol for predicting molecular bond energy. Science China Chemistry, 2019, 62, 1698-1703.	4.2	4
594	Theoretical Mechanistic Studies of Rhâ€Catalyzed C(sp 3 )—H Amination: A Comparison with Co Analogue and Metal Effects. Chinese Journal of Chemistry, 2020, 38, 1526-1532.	2.6	4

#	Article	IF	CITATIONS
595	Spatial Confinement of a Carbon Nanocone for an Efficient Oxygen Evolution Reaction. Journal of Physical Chemistry Letters, 2021, 12, 2252-2258.	2.1	4
596	Electric Field Controlled Single-Molecule Optical Switch by Through-Space Charge Transfer State. Journal of Physical Chemistry Letters, 2021, 12, 9094-9099.	2.1	4
597	A PCA-LSTM-Based Method for Fault Diagnosis and Data Recovery of Dry-Type Transformer Temperature Monitoring Sensor. Applied Sciences (Switzerland), 2022, 12, 5624.	1.3	4
598	Nonadiabatic Histidine Dissociation of Hexacoordinate Heme in Neuroglobin Protein. Journal of Physical Chemistry A, 2010, 114, 1980-1984.	1.1	3
599	Exploring concerted effects of base pairing and stacking on the excitedâ€state nature of DNA oligonucleotides by DFT and TDâ€ÐFT studies. International Journal of Quantum Chemistry, 2011, 111, 2366-2377.	1.0	3
600	Potentialâ€induced Raman behavior of individual ( <i>R</i> )â€diâ€2â€naphthylprolinol molecules on a Agâ€modified Ag electrode. Journal of Raman Spectroscopy, 2011, 42, 951-957.	1.2	3
601	The equilibrium geometry of A@C60: A test case for conventional density functional theory. Chemical Physics Letters, 2014, 591, 312-316.	1.2	3
602	Hydrophobicity and Hydrophilicity Balance Determines Shape Selectivity of Suzuki Coupling Reactions Inside Pd@meso-SiO <sub>2</sub> Nanoreactor. Journal of Physical Chemistry C, 2016, 120, 10244-10251.	1.5	3
603	UV gelation of single-component polyacrylates bearing dinitrobenzoate side groups. Chemical Communications, 2016, 52, 9383-9386.	2.2	3
604	A computational study of the reactivity of rare-earth/phosphorus Lewis pairs toward polymerization of conjugated polar alkenes. Inorganic Chemistry Frontiers, 2020, 7, 4600-4610.	3.0	3
605	A computational study of isoprene polymerization catalyzed by iminopyridine-supported iron complexes: Ligand-controlled selectivity. Chemical Physics Letters, 2020, 755, 137811.	1.2	3
606	Benchmark study of density functionals for the insertions of olefin and polar monomers catalyzed by α–diimine palladium complexes. Computational and Theoretical Chemistry, 2020, 1187, 112942.	1.1	3
607	Theoretical Spectroscopic Studies on Chemical and Electronic Structures of Selenocysteine and Pyrrolysine. Journal of Physical Chemistry A, 2020, 124, 2215-2224.	1.1	3
608	Firstâ€Principles Study on the Molecular Mechanism of Solarâ€Driven CO <sub>2</sub> Reduction on Hâ€Terminated Si. ChemSusChem, 2020, 13, 3524-3529.	3.6	3
609	Bridged Azobenzene Enables Dynamic Control of Through-Space Charge Transfer for Photochemical Conversion. Journal of Physical Chemistry Letters, 2021, 12, 3868-3874.	2.1	3
610	Structure-Based Relative Energy Prediction Model: A Case Study of Pd(II)-Catalyzed Ethylene Polymerization and the Electronic Effect of Ancillary Ligands. Journal of Physical Chemistry B, 2021, 125, 12047-12053.	1.2	3
611	Characterization of a novel broad-spectrum endolysin PlyD4 encoded by a highly conserved prophage found in Aeromonas hydrophila ST251 strains. Applied Microbiology and Biotechnology, 2022, 106, 699-711.	1.7	3
612	Multivariate Linear Regression Models to Predict Monomer Poisoning Effect in Ethylene/Polar Monomer Copolymerization Catalyzed by Late Transition Metals. Inorganics, 2022, 10, 26.	1.2	3

#	Article	IF	CITATIONS
613	Ring-opening polymerization of l-lactide catalyzed by food sweetener saccharin with organic base mediated: A computational study. Polymer, 2022, 246, 124747.	1.8	3
614	Temporal and Spatial Effects of Urbanization on Regional Thermal Comfort. Land, 2022, 11, 688.	1.2	3
615	Mechanistic Studies on Nickel-Catalyzed Ethylene Polymerization: Ligand Effects and Quantitative Structure–Activity Relationship Model. Organometallics, 2022, 41, 3212-3218.	1.1	3
616	Modulation of supercontinuum generation and formation of an attosecond pulse from a generalized two-level medium. Journal of Physics B: Atomic, Molecular and Optical Physics, 2007, 40, 1523-1534.	0.6	2
617	First-principles calculations of adsorption and dehydrogenation of trans-2-butene molecule on Pd(110) surface. Journal of Chemical Physics, 2009, 131, 154703.	1.2	2
618	Role of the <sup>3</sup> (ππ*) State in Photolysis of Lumisantonin: Insight from ab Initio Studies. Journal of Physical Chemistry A, 2011, 115, 7815-7822.	1.1	2
619	Understanding the Influence of Guest–Host Interactions on the Conformation of Short Peptides in a Hydrophobic Cavity: A Computational Study. ChemPhysChem, 2011, 12, 1325-1333.	1.0	2
620	Thermal effects on electronic properties of CO/Pt(111) in water. Physical Chemistry Chemical Physics, 2013, 15, 13619.	1.3	2
621	Study of the Electronic and Optical Properties of Hybrid Triangular (BN)xCy Foams. Journal of Physical Chemistry C, 2014, 118, 22181-22187.	1.5	2
622	Highly efficient and controllable method to fabricate ultrafine metallic nanostructures. AIP Advances, 2015, 5, 117216.	0.6	2
623	H–H and N–H Bond Cleavages of Dihydrogen and Ammonia by a Bifunctional Imido (NH)-Bridged Diiridium Complex: A DFT Study. Organometallics, 2017, 36, 4721-4726.	1.1	2
624	DBU and TU synergistically induced ring-opening polymerization of phosphate esters: a mechanism study. New Journal of Chemistry, 2021, 45, 1953-1958.	1.4	2
625	Computational insights into Ir( <scp>iii</scp> )-catalyzed allylic C–H amination of terminal alkenes: mechanism, regioselectivity, and catalytic activity. RSC Advances, 2021, 11, 19113-19120.	1.7	2
626	Macrolides mediate transcriptional activation of the <i>msr</i> (E)- <i>mph</i> (E) operon through histone-like nucleoid-structuring protein (HNS) and cAMP receptor protein (CRP). Journal of Antimicrobial Chemotherapy, 2022, 77, 391-399.	1.3	2
627	Theoretical mechanistic insights into dinitrogen cleavage by a dititanium hydride complex bearing PNP-pincer ligands. Dalton Transactions, 2022, 51, 918-926.	1.6	2
628	Observing Two-Dimensional Spontaneous Reaction between a Silicon Electrode and a LiPF <sub>6</sub> -Based Electrolyte <i>In Situ</i> and in Real Time. Journal of Physical Chemistry Letters, 2022, , 3224-3229.	2.1	2
629	NaCl salinity enhances tetracycline bioavailability to Escherichia coli on agar surfaces. Chemosphere, 2022, 302, 134921.	4.2	2
630	Exploring at nanoscale from first principles. Frontiers of Physics in China, 2009, 4, 256-268.	1.0	1

#	Article	IF	CITATIONS
631	Stable High-Energy Density Super-Atom Clusters of Aluminum Hydride. Chinese Journal of Chemical Physics, 2012, 25, 147-152.	0.6	1
632	First-principles investigations on the anisotropic charge transport in 4,4′-bis((E)-2-(naphthalen-2-yl)vinyl)-1,1′-biphenyl single crystal. Theoretical Chemistry Accounts, 2014, 133, 1.	0.5	1
633	A theoretical study on single-electron reduction of a thiolate-bridged diiron diazene complex. Chemical Physics Letters, 2015, 639, 300-303.	1.2	1
634	Computational studies on the effects of substituents on the structure and property of zinc dialkyldithiophosphates. Computational and Theoretical Chemistry, 2017, 1099, 195-202.	1.1	1
635	Harvesting of surface plasmon polaritons: Role of the confinement factor. Journal of Chemical Physics, 2020, 153, 094107.	1.2	1
636	Recurrent fever of unknown origin: An overlooked symptom of Fabry disease. Molecular Genetics & Genomic Medicine, 2020, 8, e1454.	0.6	1
637	The correct assignment of vibrationally-resolved absorption spectra of protonated anthracene isomers. Spectrochimica Acta - Part A: Molecular and Biomolecular Spectroscopy, 2021, 244, 118832.	2.0	1
638	Phononic Fine-Tuning in a Prototype Two-Dimensional Hybrid Organic–Inorganic Perovskite System. Journal of Physical Chemistry Letters, 2022, 13, 5480-5487.	2.1	1
639	A multi-dimensional microcanonical Monte Carlo study of S0 → T1 intersystem crossing of isocyanic acid. Science in China Series B: Chemistry, 2009, 52, 1885-1891.	0.8	0
640	Simulation of electronic structure of nanomaterials by central insertion scheme. Frontiers of Physics in China, 2009, 4, 307-314.	1.0	0
641	Feasible Catalytic Strategy for Writing Conductive Nanoribbons on a Single-Layer Graphene Fluoride. Journal of Physical Chemistry C, 2014, 118, 22643-22648.	1.5	0
642	Rücktitelbild: Visualization of Vibrational Modes in Real Space by Tipâ€Enhanced Nonâ€Resonant Raman Spectroscopy (Angew. Chem. 3/2016). Angewandte Chemie, 2016, 128, 1232-1232.	1.6	0
643	Landslide and Debris Flow Hazard Risk Analysis and Assessment in Yunnan Province. , 2018, , .		0
644	THU0593â€CLINICAL AND GENETIC FEATURES OF CHINESE ADULT PATIENTS WITH TUMOR NECROSIS FACTOI RECEPTOR-ASSOCIATED PERIODIC SYNDROME. , 2019, , .	5	0
645	First-Principles Observation of Bonded 2D B4C3 Bilayers. ACS Omega, 2021, 6, 13218-13224.	1.6	0